Micro/nanofluidics enabled biomedical devices: Integration of structural design and

manufacturing

Mengtian Yin, Zachary Alexander Kim, and Baoxing Xu*

M. Yin, Z. A. Kim, B. Xu

Department of Mechanical and Aerospace Engineering, University of Virginia, Charlottesville,

VA 22904, USA

*E-mail: bx4c@virginia.edu

Keywords: micro/nanofluidic devices; structural design; manufacturing; biomedical applications

Micro/nanofluidic devices and systems have attracted ever-growing attention in healthcare applications over the past decades due to low-cost yet easy-customizable functions with the demand of only a small volume of sample fluid. The continuous development, in particular, supported by the emergence of new materials, capable of meeting critical needs in next-generation, wearable, and multifunctional biomedical devices for at-home, personalized healthcare monitoring is challenging the principles and strategies of structural design, manufacturing, and their seamless integration. This review summarizes the progress in micro/nanofluidics enabled biomedical devices with a focus on structural design, manufacturing, and applications in healthcare. Structures of fluidic channels and liquid actuation strength are given to elucidate the manipulations and controls of fluid transports that help capture desirable information of interest, including component separation, extraction, measurements, and disease diagnoses. Manufacturing processes of fluidic devices in micro and nanoscales and their basic working principles are also presented, ranging from lithography in traditional hard materials to 3D printing in emerging soft materials. The selected examples and demonstrations are illustrated to highlight applications of biomedical fluidic devices in a broad variety of disease detection and diagnosis. The associated challenges and future opportunities are discussed.

1

1. Introduction

Biomedical devices and systems have attracted increasing interest because of the elevated demand of portable, accessible and highly reliable applications in healthcare over the past decades. [1] Traditional biomedical devices and systems are usually constrained by high cost and long-time diagnosis, low efficiency and accessibility, and poor mobility. [2] Numerous solutions and devices have been developed in structural design and manufacturing across different length scales with employments of different materials, including micro-electromechanical systems (MEMS), [3] electrochemical biosensor, [4] and flexible electronics. [5] Given that most biomarkers can be detected and diagnosed through body fluids such as sweat, blood and urine, micro/nanofluidic devices and systems that enable transport liquid in a well-controlled manner offer an attractive platform in biomedical engineering and healthcare applications. In these fluidic devise and systems, only a small volume of samples is needed for analysis while still providing high resolution and sensitivity because of micro/nano scale of nature. Besides, compared with MEMS technology that relies heavily on a complex manufacturing process such as high-cost lithography, the design and manufacturing of fluidic biomedical devices possess merits of low-cost and high flexibility. [6]

One of the very first microfluidic biomedical devices could be traced back to the development of a polymerase chain reaction (PCR) in continuous flow at high speed on a glass chip.^[7] The success of this chip opened up areas of microfluidic devices to efficiently amplify DNA with faster heating cycle in medical diagnostics. In the late 1990s an elastomer known as polydimethylsiloxane (PDMS) became prevalent as its properties include biocompatibility, optical transparency, and low manufacturing costs compared to conventional hard materials such as glad and silicon.^[8] An example of advancement in microfluidic devices has been the development of organ-on-chips which can grow cells in chambers to model physiological functions of tissues and organs.^[9] Recently, a flexible wearable device has been designed for sweat capture.^[10] This device was able to provide a wireless communication of onsite colorimetric results showing biomarkers of chloride and hydronium ions, glucose, and lactate. Similar microfluidic devices that combine standard droplet microfluidics to allow for fluidic operations in tests for culturing and sorting of yeast cells has also been developed. This device design demonstrated that droplet generation, encapsulation, merging, mixing, trapping, incubation, sorting, and on-demand volume tuning could be conducted in a single chip with compact design.^[11] With the development of advanced

materials synthesis and manufacturing techniques at the nanoscale over the past years, nanopores and channels have been leveraged to transport biofluids, and devising such nanofluidic devices for high controllability are expected to revolutionize biomedical applications. Different from the microfluidic devices with an in-plane design of pores and channels, in most recent years, 3D microfluidic devices are emerging to mimic complex biofluidic networks and even reproduce them for organ regenerations. For example, a 3D blood-brain barrier microvascular network has been designed to replicate in vivo neurovascular organization. The continuous demands of fluidic devices and systems toward multifunctionalities, low cost and user-friendly features capable of meeting accuracy, complexity and high efficiency of diagnoses in biomedical engineering and healthcare are challenging the conventions and strategies of devices and systems from structural design to manufacturing and to their integrations across different length scales with a broad variety of materials.

This work aims to provide a comprehensive review of micro/nanofluidics enabled biomedical devices and systems including the structural design, material selection, fabrication techniques and representative applications in biomedical engineering and healthcare. Section 2 is focused on structural designs of devices and power sources of fluid actuation. In section 3, the progress of advanced manufacturing technologies for producing biomedical fluidic devices are provided and discussed. Typical materials used for microfluidic devices including the traditional hard materials of glass and silicon and newly emerged soft materials are classified in terms of their manufacturing scale and mechanical property of elastic modulus. A broad variety of fabrication and manufacturing approaches are presented, and in particular, a series of 3D printing technologies and their modification for specific materials and structural designs are discussed. Nanofabrication is introduced to highlight its unique features and abilities brought by its extreme small scale and the associated processing difficulties. Section 4 exemplifies the representative applications of fluidic devices in biomedicine and healthcare, including biomolecular analysis, extraction, separation, and testing and the sensing and detection of biomarkers for disease diagnosis and healthcare monitoring. A brief summary, along with the challenges and opportunities, is provided in Section 5.

2. Structural designs of microchannels and actuation power source

2.1. Structural design: from 1D to 3D channels

The design of microfluidic devices is the very first, but also the most fundamental step in the whole development process. The complexity of microfluidic devices here is classified as 1D, 2D, 3D microstructures. Figure 1 shows various structural designs of microfluidic devices, based on their geometry. Straight channel microfluidic devices are the simplest design of channels [Figure 1A]. They have one straight microchannel with one inlet and one outlet. Due to their simple function, microfluidic devices with straight channels are generally used to evaluate material compatibility between injected objects and their devices. Similar device designs with cells coated on channels have also been used in cell culture to study organ-specific toxicity in humans. [14] Different from the straight channels, spiral channels have also been devised in microfluidic devices to help separate or sort particles by leveraging the inertia of flow.^[15] For example, Figure 1B shows a multiplexing slanted microfluidic device with spiral channels. A blood sample is injected into the microfluidic device from a syringe, and then flows through spiral microchannels to separate blood plasma with the inertial forces generated. Red blood cells and white blood cells are concentrated near the inner wall, and blood plasma is collected from the outer wall. Y-channel microfluidic devices have been used for liquid mixing or particle separation on the basis of controlling the direction of flow due to their simple yet practical function. [16] Figure 1C shows cryoprotectant (CPA) solutions with different concentrations being injected from inlet 1 (blue) and 2 (red) and mixed together in the green region. Mixed liquid meets oocytes injected from cell inlet C₁₃ and finally flows to outlet O₃ to allow oocyte retrieval. These representatives of microfluidic devices are designed with the 1D flow mechanism, where both the input and output channels are integrated on the same plane.

Microfluidic devices could also stack microchannels layer by layer to allow interaction of liquid flow between each layer. **Figure 1D** is a lung-on-a-chip microdevice that uses separated PDMS microchannels to form an alveolar-capillary layer on a PDMS membrane with a coated extracellular matrix (ECM). Physiological breathing movements are recreated by applying a vacuum to the side chambers, and the mechanical stretching of the PDMS membrane helps form the alveolar-capillary layer. **Figure 1E** is a placenta-on-a-chip that recapitulates the multilayered 3D architecture of the placental barrier. Trophoblast and endothelial cells are cocultured on the opposite sides of a thin porous polymeric membrane. Exchange of material through the placental

barrier is enabled by the concentration gradient between the top and bottom liquid flow. These devices are often referred to as organ-on-a-chip because a culture of organ tissues between layered microchannels is designed to mimic the function of human organs. Numerous similar organ-on-a-chip microfluidic devices have been developed to improve the design integration of multilayer structures over the recent years.^[17]

Further extension of multilayer microfluidic devices is enabled by the design of 3D channels. For example, **Figure 1F** shows a 3D microfluidic device driven by capillary force has been developed, named 3D μPAD. This device demonstrates great success to test up to 4 different samples for 4 different analytes, and enables to display results side-by-side for straightforward comparison. **Figure 1G** shows a 3D printed microfluidic device with a microneedle attached at the bottom. The design of 3D spiral mixing channels allows to mix red and blue liquids and flow to a hollow microneedle array outlet. With the assistance of 3D printing technology, 3D microchannel becomes one of the most popular design choices nowadays.^[18]

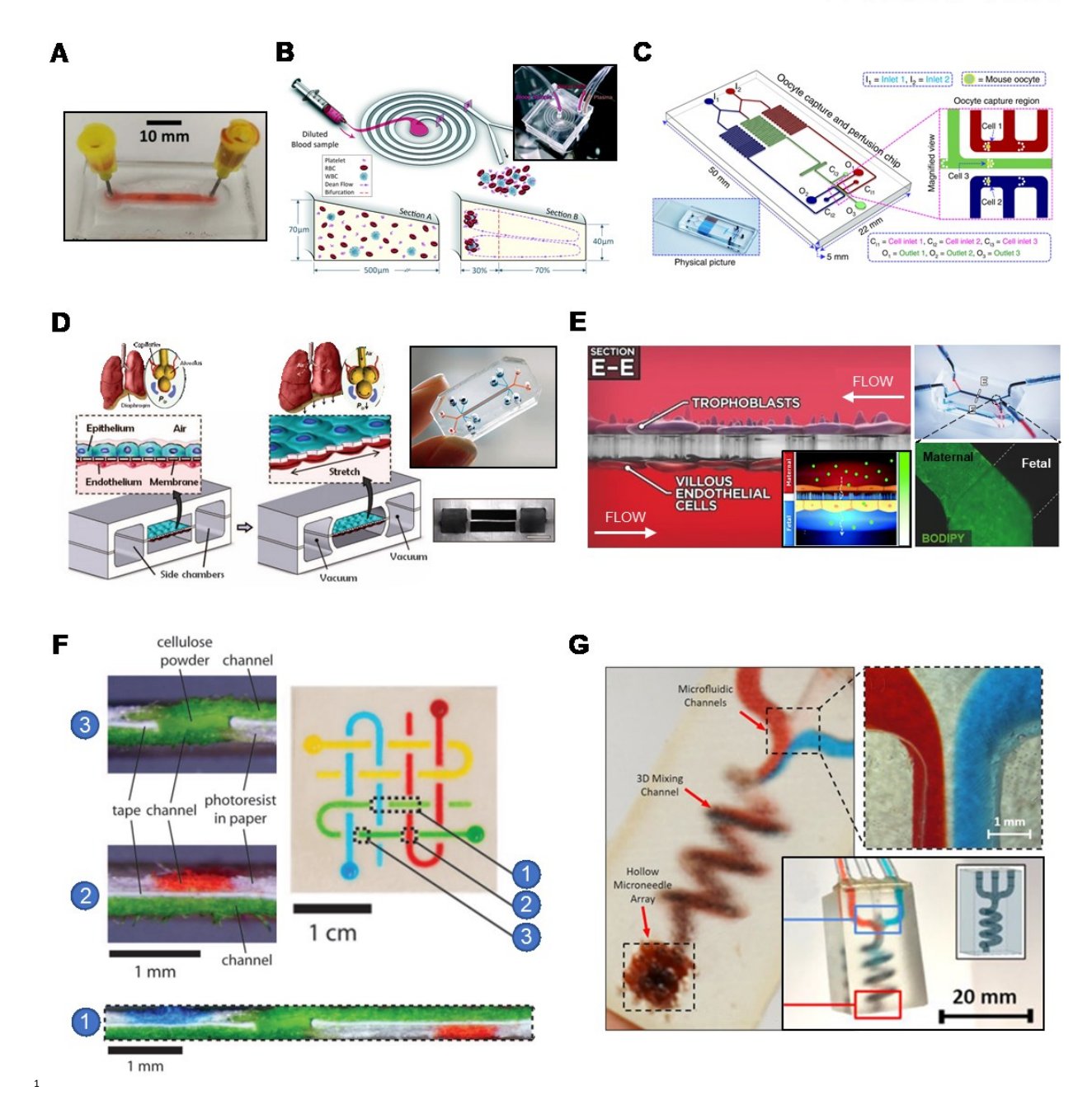


Figure 1. Structural design of microfluidic devices. A. Microfluidic device design with typical straight channels. Reproduced with permission.^[19] Copyright 2018, Institute of Electrical and Electronics Engineers. B. Device design with multiplexing slanted spiral microchannels. Section-views at the bottom reflect the distribution of blood plasma right after entering the spiral channel and before leaving. Inset at the upper right corner is the optical image of the device. Reproduced with permission.^[20] Copyright 2016, Royal Society of Chemistry. C. Y-channel microfluidic device used for liquid mixing. Inset is the optical image of the microfluidic chip. Reproduced with

permission.^[21] Copyright 2020, Springer Nature. **D.** Multilayer microfluidic device design that allows air exchange with mechanical expansion and contraction. Inlets on the right show an optical image of the microchip and a side view of microchannels. Reproduced with permission.^[22] Copyright 2010, American Association for the Advancement of Science. **E.** Microfluidic device enabled by multilayer design, where the interaction between maternal and fetal channels is driven by the gradient of concentration. Insets on the right are the optical image of a microfluidic chip and a close-up view of the connection area. Reproduced with permission.^[23] Copyright 2018, Wiley-VCH. **F.** 3D microfluidic device design with the stacking of patterned papers and double-sided adhesive tapes. Three cross-section views (1,2,3) show three independent layers of the device. Reproduced under terms of the CC-BY license.^[24] Copyright 2008, The Authors, published by American Association for the Advancement of Science. **G.** 3D microfluidic-enabled hollow microneedle device. The image in the upper right corner is the enlarged area where liquid mixes, and the one in the lower right corner shows an optical image of the device with a CAD model as inset. Reproduced with permission.^[25] Copyright 2019, American Institute of Physics.

2.2. Actuation of fluids in microchannels with outer source power

The word "microfluidic" refers to the control of fluid in a confined micro-scale device. Extensive research has been devoted to the flow of fluid through microchannels.^[26] Here we focus on the liquid flow with assistance from an outer power source. The most fundamental way is the physical interaction between the injected fluid and solid (the device) where fluids are in physical contact with the device so that a signal (mainly electrical) can be monitored.^[27] **Figure 2A** shows a microfluidic device that monitors bacterial antibiotic susceptibility. A two-layer microfluidic channel (upper left) is bonded onto a glass substrate with deposited thin film electrodes. Changes in electrical resistance of the microchannel reflect the growth and morphological changes of bacteria trapped in the microchannel and can be used to perform the rapid antibiotic susceptibility test. Biochemical interaction usually relies on the coating of enzymes, antibodies, and aptamers on microfluidic devices to detect biomarkers in the injected liquid.^[28] Electrical signals can be monitored during the chemical reaction between coatings and biomarkers. **Figure 2B** is a bead-based biosensor integrated microfluidic device for detecting cell-secreted growth factors. Cells are

cultured in the middle chamber and then permeate through the hydrogel barriers to the sensing chamber, where cells are detected with antibody-coated beads.

Electrical and magnetic fields are also powerful tools to help control the flow of liquid in microfluidic devices. [29] For instance, **Figure 2C** shows the exclusion of emulsion coalescence in microfluidic channels using an electrical field. Emulsion droplets are generated with the insertion of a glass capillary into the polymethyl methacrylate (PMMA) device on the left side. The dynamic behavior of emulsion droplets can be adjusted by changing the intensity of the electric field. Different from the utilization of electrical fields, magnetic fields are also employed to separate magnetic particles in a continuous flow microfluidic device, as shown in **Figure 2D**. When magnetic focusing is employed, all particles are captured on the attractive region, indicating a complete separation.

Heat, as an easily accessible power source, is also suitable to be used to control the flow of fluid.^[30] For example, **Figure 2E** shows the acceleration of the drug diffusion into human tissues from microneedle devices by integrating a microheater. Heat generated from the 3D printed microheater on top is delivered to microneedles underneath the PI layer and increases the release of drug from the microneedles to the epidermis. Another example of an outer power source is using acoustic waves to manipulate particles in microchannels.^[31] In **Figure 2F**, an acoustic field and acoustic streaming are generated in microchannels and used to manipulate suspended particles. Particles are levitated along the z axis, pushed together, moved along the y axis, and dropped back with a trapping node (blue circle).

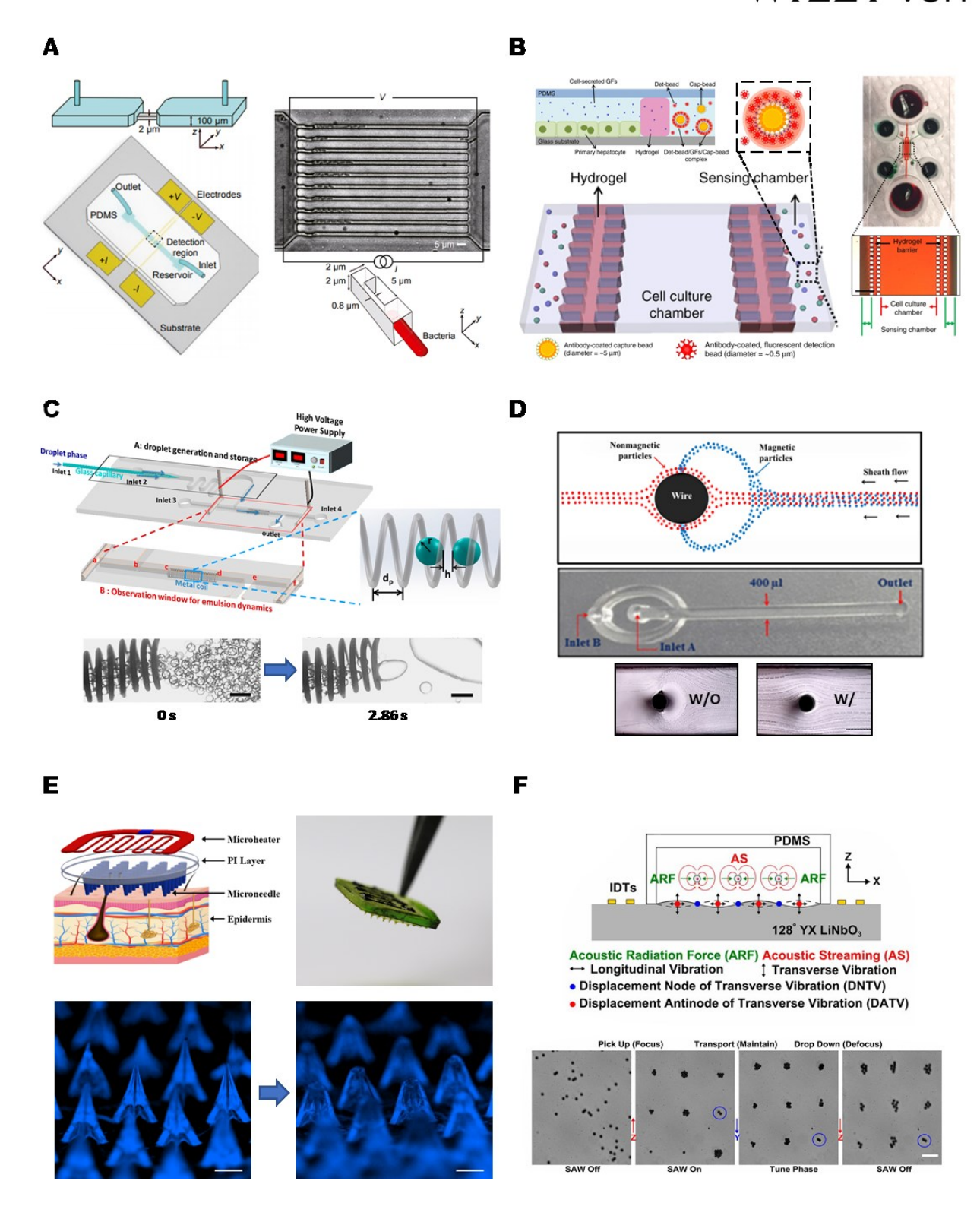


Figure 2. Outer source design with enhanced flows of liquid. A. Schematics (left) and microscope image (right) of the microfluidic device, where the physical interaction between bacteria and

PDMS chips yield electrical signals to monitor the growth of bacteria (K. pneumoniae). Reproduced under terms of the CC-BY license.^[32] Copyright 2020, The Authors, published by American Association for the Advancement of Science. B. Microfluidic device design that allows biochemical reactions between liquid samples and antibody-coated beads. Reproduced under terms of the CC-BY license. [33] Copyright 2017, The Authors, published by Springer Nature. C. Microchannel design with an electrical field for the control of emulsion. Optical images below show the influence of the electric field before (0 s) and after (2.86 s) electric field is applied. Reproduced under terms of the CC-BY license.^[34] Copyright 2015, The Authors, published by Multidisciplinary Digital Publishing Institute. **D.** Microfluidic device capable of being controlled by a magnetic field for particle separation in a continuous flow. The schematic diagram and optical image at the top show the separation of magnetic and non-magnetic particles in the presence of a magnetic field. Bottom two show local different flows of particles without and with the presence of the magnetic field. Reproduced under terms of the CC-BY license. [35] Copyright 2017, The Authors, published by IOP Publishing. E. Microfluidic needle array with enhanced fluid diffusion by the integrated microheater. An optical image of a microheater integrated microneedle patch is shown at the upper right corner. Bottom two microscopic images show morphologies of microneedle arrays before and after the microheater is turned on. Reproduced with permission.^[36] Copyright 2019, Wiley-VCH. F. Microfluidic device design the implantation of 3D acoustic tweezers for trapping and manipulating single cells and particles. The cross-section image shows the mechanism of a standing surface acoustic wave enables particle manipulation in a microfluidic chamber. The optical image at the bottom shows three-dimensional acoustic trapping and manipulation. Particles are levitated along z axis, pushed together, moved along y axis, and dropped back with a trapping node (blue circle). Reproduced with permission.^[37] Copyright 2019, Wiley-VCH.

3. Manufacturing principles and approaches

3.1. Material selection: from hard to soft materials

Once we have the design of microfluidic devices, the next step will be the fabrication. Before we actually build a template or start a 3D print, the material of choice for the microfluidic devices must be determined based on the desired application. Typical materials that are used to fabricate

microfluidic devices include metal, glass, ceramic, composite, elastomer, thermoplastic, and paper. For example, the very first microfluidic device was fabricated with silicon with traditional lithography. [38] Glass was also used as a substrate soon after that because of low costs. [39] These materials have been largely replaced with relatively soft materials like elastomers and thermoplastics to achieve biomedical applications, because silicon is relatively expensive and opaque, while glass is hard to process on a small scale. [40] Applications of microfluidic devices in the biomedical field commonly require devices to have features such as being lightweight, tolerant to mechanical deformation such as bending or twisting that can tune the flow of liquid. Figure 3 shows a guidance map for the selection of materials. The location of each bubble on the x-axis represents its Young's modulus while the location on the y-axis represents the common processing scale of the material. Young's modulus of metals and glass typically range from tens to hundreds of GPa, and are considered as hard materials.^[41] In contrast, elastomers and thermoplastics typically have Young's modulus ranging from only one to hundreds of Pa and are easy to be deformed, light, and relatively cheap, and are referred to as soft materials. For example, elastomers such as PDMS or conductive polymers can be chosen if one would like to fabricate a micro scale soft fluidic device. Going down to nanoscale devices, metals like silicon or stainless steel can be chosen to fabricate highly packed microneedle patches, with the help of standard lithography.

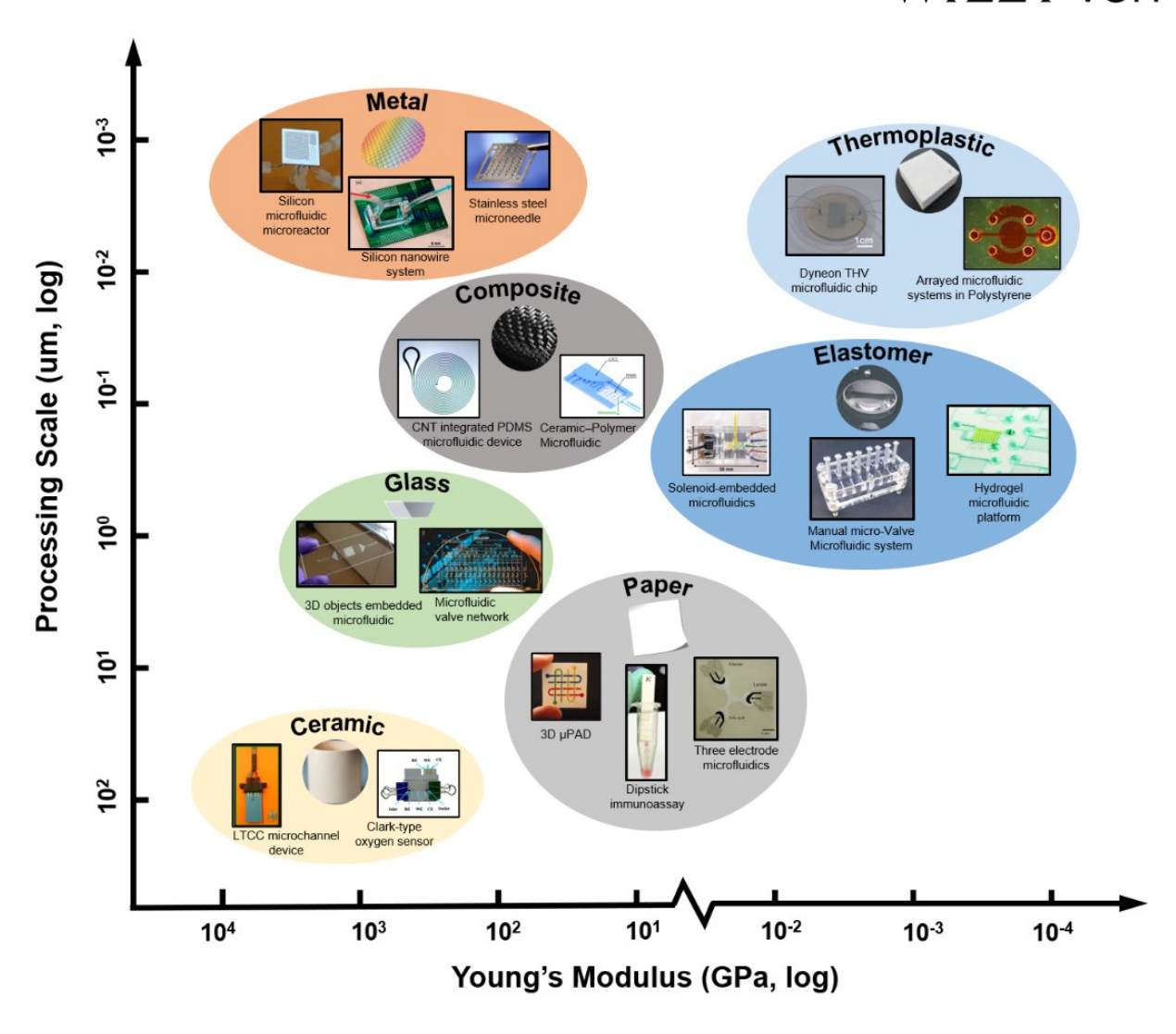


Figure 3. Guidance map for the material selection with respect to Young's modulus and processing scale. The length of each inset represents the approximated range of young's modulus on *x*-axis, while the width means the general range of processing scale. From left to right, Young's modulus of materials decreases, representing a shift from hard materials (like metals and ceramics) to soft materials (like elastomers and thermoplastics). From down to up, the processing scale decreases from 100 um level (ceramics with machining or laser melting) to 1 nm (metals with lithography), suggesting an increased difficulty of the machining process. "Dyneon THV microfluidic chip" reproduced with permission. [42] Copyright 2011, Royal Society of Chemistry. "Arrayed microfluidic systems in polystyrene" reproduced with permission. [43] Copyright 2011, Royal Society of Chemistry. "Hydrogel microfluidic platform" reproduced with permission. [44] Copyright 2014, Royal Society of Chemistry. "Manual micro-valve microfluidic system"

reproduced with permission.^[45] Copyright 2020, John Wiley and Sons. "LTCC microchannel device" reproduced with permission.^[46] Copyright 2010, Springer Nature. "Three electrode microfluidics" reproduced with permission.^[47] Copyright 2009, American Chemical Society. "Solenoid-embedded microfluidics" reproduced with permission.^[48] Copyright 2015, Elsevier. "Microfluidic valve network" reproduced with permission.^[49] Copyright 2006, Royal Society of Chemistry. "3D objects embedded microfluidic" reproduced with permission.^[50] Copyright 2019, Springer Nature. "Ceramic–Polymer Microfluidic" reproduced under terms of the CC-BY license.^[51] Copyright 2020, The Authors, published by Multidisciplinary Digital Publishing Institute. "Clark-type oxygen sensor" reproduced with permission.^[52] Copyright 2017, Elsevier. "CNT integrated PDMS microfluidic device" reproduced with permission.^[53] Copyright 2018, Springer Nature. "Silicon nanowire system" reproduced with permission.^[54] Copyright 2009, American Chemical Society. "Silicon microfluidic microreactor" reproduced with permission.^[55] Copyright 2005, Royal Society of Chemistry. "Stainless steel microneedle". Reproduced with permission.^[56] Copyright 2009, MedGadget (Internet). "Dipstick immunoassay" reproduced with permission.^[57] Copyright 2017, Elsevier.

3.2. Manufacturing methods: from molding to 3D printing

With the selection of material, proper fabrication methods can be applied to produce microfluidic devices with desired channels. Early-stage silicon-made microfluidic devices use traditional lithography including patterning, and dry and wet etching due to the high Young's modulus of silicon. Here we focus on fabrication methods related to soft materials that are nowadays mostly employed in micro/nanofluidic devices for biomedical applications. The most widely accepted fabrication method for elastomer-based microfluidic devices started with the soft lithography technique. This technique first applies lithography on the rigid substrate (typically silicon wafer) to generate the desired pattern and then elastomeric material (typically PDMS) is poured onto the patterned silicon wafer template. Finally, elastomeric microfluidic devices can be fabricated after etching templates and punching holes [Figure 4A]. Soft lithography is fast and low-cost compared to traditional lithography and is favored in laboratory-scale demonstration of devices due to its high accessibility. Several improvements of this technique have also been developed to accommodate materials of interest and optimize the fabrication processes. [59]

Non-lithographic techniques are also developed in pursuit of simpler, cheaper, and more accessible solutions. Transfer printing technique is one of the popular representatives. It usually starts with the printing of lithographing patterns on a sacrificial substrate and then transfers to the desired substrate by peeling off patterns from the sacrificial substrate. [60] As indicated in Figure 4B, Si microneedles are peeled off from the Si wafer substrate with water-soluble film and then are attached onto the desired patch substrate. The fabricated microneedle patch has rigid microneedles for penetration through the epidermis, but a soft substrate to allow deformation with skin. A similar transfer printing technique was also adapted and named print-and-peel fabrication. [61] A PDMS stamp is reversibly adhered to a glass substrate to transfer patterns onto the glass substrate and then liquid PDMS is coated on the pattern to form a microfluidic device. Most recently, a green transfer printing technology that allows the reuse of fabrication substrates such as silicon without any chemicals is developed to fabricate 3D structures with channels, [62] and even attractively, the transfer could be conducted to pick up films from a liquid substrate for deterministic assembly of structures.^[63] Another solution of non-lithography fabrication is the laminate manufacturing method. Figure 4C shows the typical laminate fabrication process of a toner-based microfluidic device for clinical diagnostics with colorimetric detection. Three layers of thin films with the desired pattern are fabricated with laser printers (top and bottom layers), laser ablation machines (middle layer), and then laminated thermally to form microchannels. Other fabrication techniques such as wire based casting, [64] direct laser plotting have also been developed to fabricate microfluidics based biomedical devices.^[65]

Most conventional soft lithography or non-lithographic method is mainly focused on devices with 2D microstructures. [66] With the increasing need for biomedical microfluidic devices, there is a significant demand for 3D structured microfluidic devices. 3D printing offers a solution to meet this requirement. More specifically, 3D printing can fabricate 3D structures using a precisely described computer-assisted designs (CAD) model, and thus has great attractions in the fabrication of biocompatible microfluidics. [67] Additive manufacturing techniques that are frequently used in the fabrication of microfluidic devices include fused deposition modeling (FDM), multi jet modeling (MJM), and stereolithography (SLA). [68] FDM 3D printing extrudes thermoplastic materials through a heating unit on a motorized nozzle [Figure 4D]. The material is solidified immediately after extrusion. One great advantage of FDM 3D printing is the wide range of material selection, including many cheap and biocompatible materials like acrylonitrile

butadiene styrene (ABS), polyethylene terephthalate (PET), poly-lactic acid (PLA), etc.^[69] **Figure 4E** shows an MJM, or polyjet modeling based 3D printing technique. It prints liquid photopolymer with a motorized inkjet head and is polymerized by UV light immediately after extrusion. One of the most remarkable strengths of MJM is that multiple materials can be printed at the same time, which makes it an ideal fabrication method for printing microfluidic devices with combined hard and soft materials.^[70] Stereolithography creates a 3D solid part with a focused laser induced crosslinking from a resin precursor, as shown in **Figure 4F**. SLA 3D printing is known by its fast printing rapid and high resolution. SLA techniques could also help fabricate microfluidic devices down to micron levels, although a sacrifice of printing time is inevitable.^[71] Insets in Figure 4D, E, F highlight typical microfluidic devices fabricated with FDM, MJM, SLA respectively.^[72]

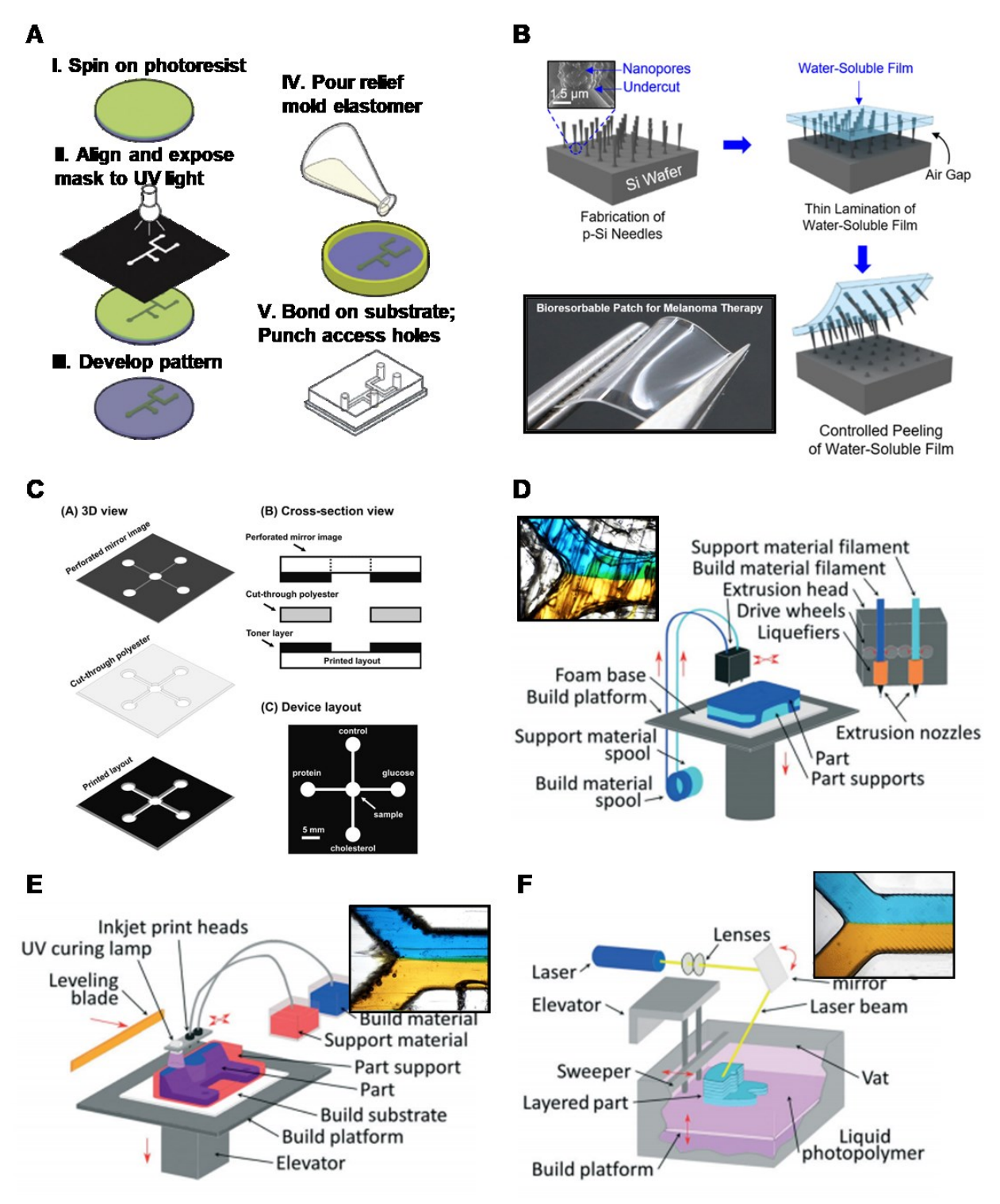


Figure 4. Fabrication methods for microfluidic devices. **A.** Fabrication process of soft lithography. Reproduced with permission.^[73] Copyright 2017, Elsevier. **B.** Transfer printing of silicon microneedles. The inset at the lower left shows an optical image of the microneedle patch. Reproduced with permission.^[74] Copyright 2020, American Chemical Society. **C.** Laminate

manufacturing method. Reproduced with permission.^[75] Copyright 2012, American Chemical Society. **D.** Schematic of typical fused deposition modeling (FDM) 3D printing. Inset shows a microscopic image of microchannels fabricated with FDM. Reproduced with permission.^[76] Copyright 2008, Custom Part Net. **E.** Schematic of multi jet modeling (MJM) 3D printing and microscopic image of microchannel fabricated with MJM (inset). Reproduced with permission.^[77] Copyright 2008, Custom Part Net. **F.** Schematic of stereolithography (SLA) 3D printing. Inset shows a microscopic image of a microchannel fabricated with SLA. Reproduced with permission.^[78] Copyright 2008, Custom Part Net.

3.3. Modifications of 3D printing for integration with structural design

3D printing is a promising technique for microfluidic manufacturing as it can make traditionally complex designs accurately and relatively cheaper and supports customizable designs. [79]. In some circumstances, modification of conventional 3D printing is needed to accommodate the printing of new materials and designs with the integration of functional components. For example, one of the main ways to modify FDM printers is through their nozzles since they are the final part in contact with the filament before it is extruded. [80] Figure 5A shows a modified FDM printing process to build a colorimetric enzyme-linked immunosorbent assay (ELISA) to detect malaria. Different print settings including layer height, extrusion speed as well as extrusion temperature were changed to improve bonding between layers. Advancements in printer software have led to the ability of MJM printers to fill void areas with a glycerol-isopropyl alcohol mixture instead of using a sacrificial material, which reduces postprocessing time. [81] Figure 5B shows a multiple flow controller which increases the number of valves for in-chip automation and reduces issues with microfluidic interconnects. The process uses a perfusion controller and a single gate pressure to limit the source to drain fluid flow and to control four different fluidic transistors. A modified type of SLA printing is volumetric SLA, which forms 3D structures as a whole unit instead of layer by layer. A volumetric SLA system uses three orthogonal beams projected into a photosensitive resin and irradiated to make 3D models.^[82] Figure 5C shows another modified SLA printer with a custom digital light processor and resin. This light engine helps create a smaller void size and a UV LED light which allows for different materials when creating resin. With this modification, the printed cross sections could be as small as 18 μ m \times 20 μ m.

In addition to the three main methods of 3D printing (FMD, MJM, and SLA) there are other modified 3D printing methods. Figure 5D shows a low-cost technique so-called laminated object manufacturing (LOM), where layers of materials are first laminated together using heat and pressure and then precisely cut by a computer-controlled system.^[83] The LOM technique is easy to use, cheap, fast, and can handle relatively large-size objects.^[84] Figure 5E shows a printing method without the need for sacrificial materials by precisely extruding inks into self-supporting microchannels. Removal of sacrificial materials allows for a reduced post-processing time, and microfluidic structures such as pumps, mixers, and channels can be directly aligned onto substrates. To create these hollow structures, it is worth noting that the maximum stress within the self-supporting structures must be less than the yield strength of the extruded ink. [85] Figure 5F shows a two-photon polymerization technique that uses a high power femtosecond pulse laser operating at a high absorption wavelength. This technique depends on the light intensity, and the required amount can only be found near the focal point of the laser (voxel). The voxel can be moved so that the laser is precisely focused within a part of the photosensitive resin and thus highresolution 3D structures can be created, such as diodes in channels.^[86] Innovations to make 3D printers faster and more affordable with better resolution will continue as the design of microfluidic devices tend to be complex and multifunctional with the emergence of new materials and the integration of multiple material components.

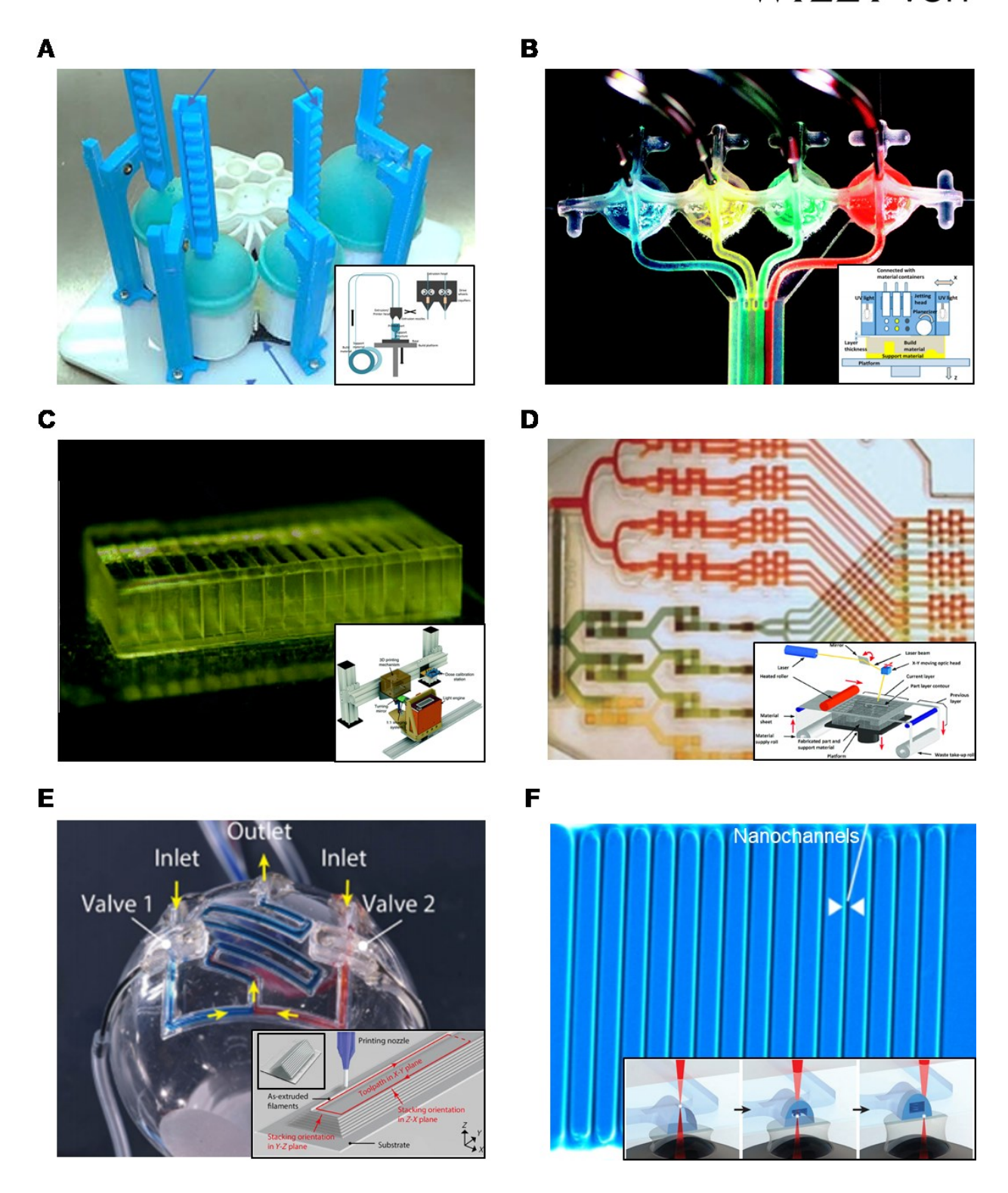


Figure 5. Enhanced 3D printing techniques for specific, on-demand designs. **A.** Modified FDM with the aim of reducing leakage in a printed fluidic platform. The inset figure shows the principle FDM printhead and material extrusion. Reproduced under terms of the CC-BY license.^[87]

Copyright 2018, The Authors, published by Multidisciplinary Digital Publishing Institute. B. Modified MJM printer with an integrated microfluidic circuits controller. The inset shows a schematic of modification. Reproduced with permission.^[70] Copyright 2016, Royal Society of Chemistry. Reproduced with permission.^[88] Copyright 2017, Taylor and Francis. C. Printed flow channels with a high aspect ratio by modified SLA printer for a custom resin and schematic of the modified SLA printer with custom resin (inset). Reproduced with permission. [89] Copyright 2017, Royal Society of Chemistry. D. Layer-by-layer assembled lamination by laser laminated combinatorial mixer. Inset shows laser lamination process. Reproduced with permission. [90] Copyright 2016, Wiley-VCH. E. Direct microchannel printing by precisely extruding into selfsupporting microchannels without requiring sacrificial materials. The main figure shows serpentine microfluidic channels with integrated valves directly printed onto the surface. Inset shows a schematic of printing directly onto the self-supporting structure. Reproduced under terms of the CC-BY license.^[91] Copyright 2020, The Authors, American Association for the Advancement of Science. F. Two-photon polymerization interfaced with conventional mask whole-wafer UV-photolithography using interaction of a femtosecond laser radiation and a highly localized chemical reaction leading to polymerization of the photosensitive material. The main figure shows printed nanochannels, while the inset shows a schematic of the femtosecond laser writing. Reproduced under terms of the CC-BY license. [92] Copyright 2019, The Authors, published by Multidisciplinary Digital Publishing Institute. Reproduced with permission. [93] Copyright 2019, The Authors, published by Springer Nature.

3.4. Fabrication of fluidic devices at the nanoscale

A nanofluidic device refers to channels or pores with at least one characteristic dimension below 100 nm.^[94] As a result, nanofluidic devices have a very high surface-to-volume ratio. exhibiting many unique features and abilities for biomedical applications. Besides, their scales can even go down to interfacial force level and are comparable to many biomolecules like proteins or DNA.^[95] Nanofluidic devices can be fabricated in many dimensions, from 0D, 1D, to 2D, and are generally referred to as nanopores, nanotubes, and nanoslits respectively.^[96] Scales of microfluidics and nanofluidics differ from hundreds to thousands of orders of magnitude and thus very different

fabrication methods are applied to ensure nanochannels not collapse or connect to each other under the influence of interfacial forces.

Currently, modified lithography techniques are still widely accepted for their high resolution and mature process in the fabrication of nanofluidic devices, where electron beam lithography (EBL), focused ion beam lithography (FIB), and nanoimprint lithography (NIL) are examples of well-developed photolithography methods.^[97] Figure 6A shows an example of NIL in the fabrication of nanofludic devices. A thin layer of imprint resist is coated onto the substrate (step 1), followed by the pressing of a nano patterned mold on the coated substrate (step 2). The pressed nanoimprint is cured by UV light or heat under the control of temperature and pressure (step 3), and then etched by plasma to expose the nanopatterned substrate (step 4). Fabricated nanochannels are then carefully sealed with polymer to enclose open channels. Figure 6B shows another approach by fabricating nanochannels directly on synthesized nanoporous material. Electro-sputtering is applied on porous alumina membrane to form gate metal layers, and subsequently performing barrier-type anodization to form a gate dielectric layer. Nanofluidic fieldeffect transistors (FET) are thus fabricated and potentially applied for DNA sequencing, drug delivery, etc. Other nanomaterials like ion selective polymer, nanotubes (1D) are also applied on the fabrication of template based nanofluidic devices. [98] The formation of nanochannels can also be assisted by water, as indicated in Figure 6C. Silica nanoparticles are tightly packed through the evaporation of water and form 0D nanopores and are applied for chemical mixing. A nanoparticle crystal fabricated with a similar capillary force-assisted assembly method is reported to produce a nanofluidic diode. [99] Figure 6D shows an energy harvest nanofluidic device fabricated with a porous carbon film. The fabrication of porous carbon film starts with two electrodes printed on the edges and a carbon nanotube slurry printed crossing electrodes. A subsequent annealing process is performed at which time the formation of nanoscale pores occurs. As water flows through porous carbon film by evaporation, a streaming current and a higher potential are created. Figure 6E is a crack-assisted nanofabrication process. Micropatterns are first fabricated on glass with lithography followed by the crack introduction onto the substrate with stress concentration/releasing structures to control the initiation, propagation, and termination. Desired nanopatterns are created after the formation of precise controlled cracks. The fabricated nanofluidic device is demonstrated with small molecules being transported. Figure 6F describes a collapse-induced formation of nanochannels, which coats a layer of PDMS on a patterned silicon substrate and then moves the

molded PDMS to a new substrate to allow self-collapse of the PDMS "roof" due to the absence of supports.

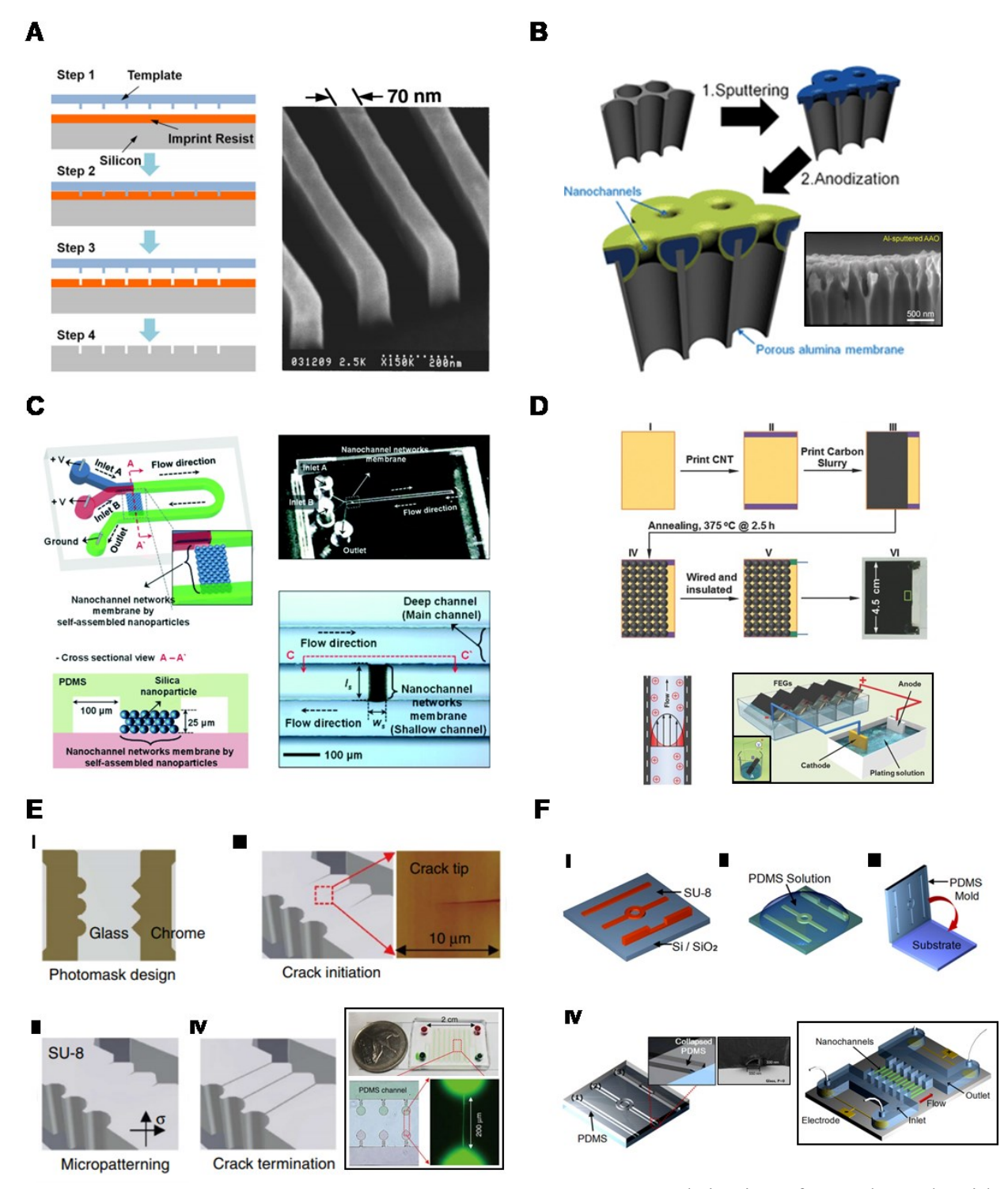


Figure 6. Fabrication approaches for nanofluidic devices. A. Fabrication of nanochannels with nanoimprint lithography. The SEM image at the right shows nanoscale channels fabricated by

nanoimprint. Reproduced with permission. [96] Copyright 2012, American Institute of Physics. B. Nanofluidic field-effect transistor (FET) fabricated with electrical sputtering. Inset is the SEM image of electrical sputtered porous alumina membrane scaffold. Reproduced with permission. [100] Copyright 2012, Royal Society of Chemistry. C. Mixer device (top) and enlarged dashed area (bottom). An active micromixer utilizes vortex generation due to non-equilibrium electrokinetics near the interface between a microchannel and assembled nanoparticle (Schematic image at left). Reproduced with permission.^[101] Copyright 2015, Royal Society of Chemistry. **D.** Nanoporous carbon film for electricity generation from water evaporation. The labeled schematic on top shows the printing process of the porous carbon film. With the evaporation-drive flow of water through the porous film, an electrical potential is generated, as shown in the schematic at the lower left corner. Schematic of the silver-microstructure fabrication device with generated electricity is shown at lower left corner, with the inset being the electricity generation unit. Reproduced with permission.^[102] Copyright 2017, Wiley-VCH. E. Crack-assisted photolithography of nanofluidic channel. Boxed image at lower right shows the nanofluidic device for the transport of small molecules, with enlarged images of channels. Reproduced with permission. [103] Copyright 2015, Springer Nature. F. Nanochannel fabrication with "roof-collapse" technique. The inset at the lower right shows the nanofluidic device for DNA elongation and nanoparticle concentration. Reproduced under terms of the CC-BY license. [104] Copyright 2009, The Authors, published by American Association for the Advancement of Science.

4. Application in biomedical engineering and healthcare

4.1. Cell analysis by fluid manipulation

Fluid manipulation techniques are an essential part of microfluidic devices as they create movement and dictate the speed of fluid and particles throughout the system. The three main basic means of fluid manipulation techniques are pumps, valves, and mixing sections. [105] Pumps are necessary for the field of microfluidics as they reduce the number of moving parts and facilitate the movement of fluid. [106] Electro-osmotic pumping relies upon an unbalanced charge distribution in the area where a fluid is in contact with a solid called the electric double layer (EDL). [107] For example, **Figure 7A** shows a pump powered by electroosmosis to facilitate the movement of fluid samples while allowing multiple flow rates and accurate injection of reagent in living cell analysis.

Valves are important in microfluidics because they are able to control both movement and flow direction in devices and have multiple designs for different uses. [108] In particular, pneumatic valves are designed to control others by sending pulses of pressure to drive fluid into channels. [109] Figure 7B shows a pneumatic valve controlling an elastomeric membrane which acts as a single microbead trap and release mechanism for selective grabbing. This trapping method can be applied to biological cells and devices, such as those involving the single-cell analysis and creating microarrays that requires high trapping ability. Mixing is the final main fluid manipulation technique which uses small channel sizes combined with variations flow to allow for mixing by diffusion. Double emulsions make microdroplets by mixing and enclosing an inner liquid with another liquid shell to be dispersed into a continuous phase. [110] These microdroplets can be used to create wound dressings by taking advantage of hydrogel's properties. [1111] Figure 7C shows a device that processes individual cells for gene sequencing by mixing barcoded hydrogel microspheres (BHM) cells, lysis reagents, and carrier oil. This device creates droplets that mix the reagents and microspheres together using the double emulsion system.

Combining these fluid manipulation techniques can lead to highly compact and sustainable yet less complicated devices. A Y-shaped mixing channel that contains two inlets has been designed to allow for input of two different samples flow into a single outlet channel. Burst valves are also used. It works by storing pressure at the outlet of cross sectional flow channels, and then bursting once the fluid front is broken when pressure is above a critical capillary pressure.^[112] Figure 7D shows a push and burst valve system and Y-shaped mixing channel to create a capillary driven simultaneous power free inflow system. The combination of these designs can be used to produce tailored concentration profiles, and specifically to tune flow rates. Oftentimes in microfluidic devices, a fluid flow must be delayed at a certain location to allow samples adequate time to react with reagents such as in blood protein analysis chips. [113] Figure 7E shows a dropletbased device for single-cell isolation, cultivation, and analysis in microorganisms. This device uses a T-shaped junction to facilitate encapsulation of cells, similar to the emulsion system in Figure 7C. Parallel channels and the shunting effect were used to slow cells down. The shunting effect occurs when ionic currents are forced through conductive paths. [114] It also implements an off-chip solenoid valve suction section which allows for rapid sorting of droplets when paired with a microcontroller.[115] This droplet based device allows for a single-cell genomic DNA amplification and sequencing, identification of microorganisms, and cultivation. Traditional trapping techniques

are another form of fluid manipulation and include electrical, optical, thermal, magnetic, and acoustic. [116] **Figure 7F** shows a device using an automated fluid flow for the fine manipulation of micro- and nanoscale particles and particle trapping. This flow control device consists of a fluidic layer (red) and a control layer (black). The fluidic layer has four buffer streams and two perpendicular microchannels to form the junction for a sample stream. Two membrane valves control the inlet and outlet stream flow rate and provide 2D control of the stagnation point. The device is made up of two layers to accommodate the membrane valves which provide superior control. [108b]

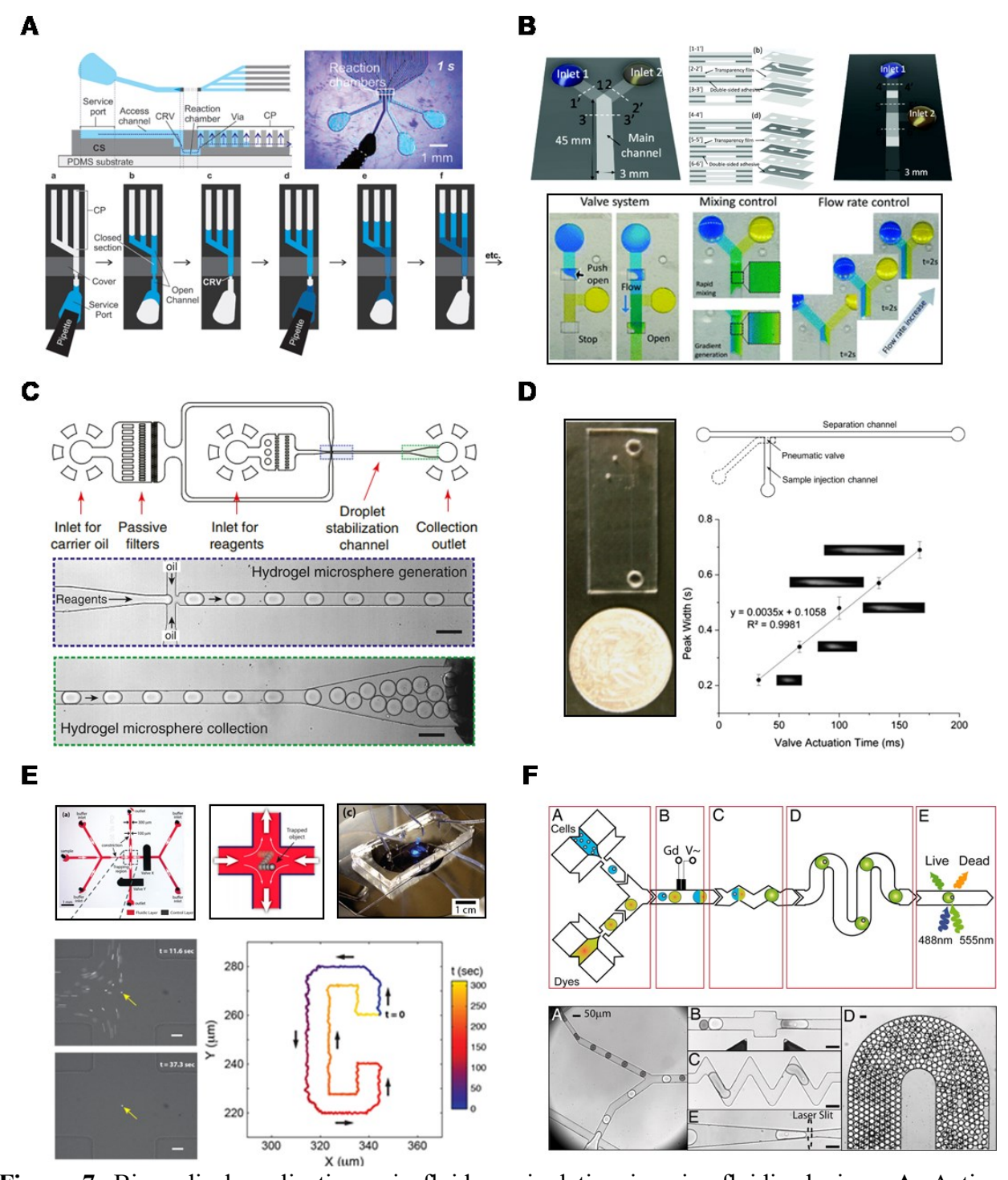


Figure 7. Biomedical applications via fluid manipulation in microfluidic devices. **A.** Active electro-osmotic (EO) pump with continuous medium perfusion for cell culture living analysis. The top figure shows the system with two cell culture lines each with one cell chamber. The bottom schematic is a diagram of the EO pump design and images of specific fabricated components. Reproduced with permission.^[117] Copyright 2009, Elsevier. **B.** Microfluidic system controlled by

pneumatic valves for microbead arraying and microarray repeatability. The top schematic shows the device structure. The bottom figure shows high speed images of microbead arrays going through a bypassing and trapping process. Reproduced with permission.^[118] Copyright 2013. Springer Nature. C. Droplet based microfluidic device to process individual cells for gene sequencing. The top figure is a schematic for the device used to barcode hydrogel microspheres (BHM). The middle figure shows each DNA droplet being synthesized with carrier oil. The bottom figure shows microspheres traveling through the stabilization channel after being broken off and into the collection outlet. Reproduced with permission.^[119] Copyright 2015, Cell Press. **D.** Flow control with capillary forces in point of need diagnostics. The top left figure shows a Y shaped channel. The top right figure shows the power free simultaneous inflow push and burst valve system. The top middle figure shows multilayer channel geometries for both the Y shaped channel device and valve system. The bottom left figure shows a schematic of the push and burst valve each opening to create a single flow. The bottom middle and left schematics show the Y shaped channel during mixing and flow rate control. Reproduced with permission. [120] Copyright 2021, Royal Society of Chemistry. E. Facile droplet microfluidic device for single-cell cultivation and microorganism analysis. The top schematic shows the layout of the entire device and the isolation process. The bottom images show parts of the isolation process. Reproduced under terms of the CC-BY license. [121] Copyright 2017, The Authors, published by Springer Nature. F. Droplet-based microfluidic technology that allows for screening and encapsulation of single mammalian cells. Section A is a set of 2 nozzles with encapsulated cells of live and dead fluorescent dyes. Section B is a fusion module that delivers an AC field to electrically merge both dyes. Section C is a rapid mixing module. Section D is a delay line for cell staining through on-chip incubation. Section E is a detection module to collect the fluorescent signals excited with a laser slit. Reproduced with permission.^[122] Copyright 2013, American Chemical Society.

4.2. Biomolecule extraction, separation, and detection in microchannel

As the field of microfluidic devices continues to progress and provide fast, inexpensive, and more portable devices, sample treatment that provides a combination of the extraction, separation, and testing of desired samples becomes more readily accessible. Through the use of microfluidic channels and fluid analysis, sample treatment processes allow the users to have rapid test results

in resources-limited settings in a wide range of biomedical applications. For example, DNA is an important biomarker to be treated because it tells a breadth of information about the body. A common DNA sample treatment method utilizes polymerase chain reaction (PCR) tests to amplify DNA results. Figure 8A shows a PCR chip designed to eliminate the use of an external pump, where the capillary driven self-propelled microchannels are introduced to amplify both DNA and Escherichia coli (E. coli). The chip was also integrated with a fluorescent detection system to observe the samples using a laser and photomultiplier tube (PMT). DNA hybridization is the process of combining self-complementary single stranded DNA or RNA molecules.^[123] Hybridization can be used in parallel with nucleic acid probes to detect the presence of certain DNA molecules in a cell. Figure 8B utilizes this method of hybridization as well as PCR testing to create a lab on a chip that yields colorimetric results for bacteria detection. After PCR amplification, the fluid is mixed with a hybridization reagent and probes detected the presence of bacteria including E. coli, Enterococcus faecalis, Klebsiella pneumoniae, etc. To create the colorimetric result, fluorescent signals were generated by probes and analyzed. Another example of a device that uses both PCR and hybridization detection methods is for mutation detection in inherited arrhythmic diseases.[124]

Blood provides a wealth of knowledge about the human body as it delivers nutrients, transports cells, and moves waste throughout the body. [125] A challenge with traditional blood analysis techniques is that it requires larger samples, high quality equipment, and long analysis time. [126] **Figure 8C** shows a self-powered microfluidic device to extract white and red blood cells from whole blood samples. This device simplifies the blood treatment process by only requiring 5µL of blood, and uses a filter trench to prepare cells for detection with a fluorescent scanner. The filter trench works when gravity pulls filtered blood cells down from the whole blood. **Figure 8D** uses tissue samples and blood to sample estradiol for breast cancer. The device integrates tissue-liquid extraction and an immunoassay to measure and quantify the amount of estradiol from core needle biopsy samples. This microfluidic device utilizes digital microfluidics (DMF) for precise control reagents, solvents, and the sample. DMF is different from channel microfluidics because it allows for individual sample droplet manipulation. [127] This device design in blood analysis includes the detection of exosomes that are released by tumor and non-malignant cells and provides information on cell origins. [128]

With the employment of microfluidic devices, sample treatment also revolves around the investigation of the physical and chemical properties of cells. Endothelial cells (EC) undergo hemodynamic forces due to pulsing blood flow and shear stress which lead to mechanical strain. [129] For instance, circulating tumor cell (CTC) adhesion coupled with a layer of endothelial cells can help understand the fundamental nature of CTC in the mechanisms of metastasis. [130] **Figure 8E** shows the exploration of the effect of hemodynamic forces, fluid shear stress, and cyclic stress to understand the cardiovascular system and relevant diseases that occur. This device utilized an elastic membrane to allow for sample storage, and a vacuum to create stretch forces on an environment of cells. The study of brain cells has originally been limited, but culturing cells to mimic brain cell behavior is a way to study the pathogenesis of brain diseases. [131] However, the growth of biofilms is often a common issue when culturing cells. **Figure 8F** utilizes a bioreactor to grow, track, and image brain organoids with a culture medium input, four outlets for each well, and an incubator environment for organoid growth. Each well was also designed for culture media replacement through the use of a solenoid valve to independently choose each well and prevent biofilm buildup.

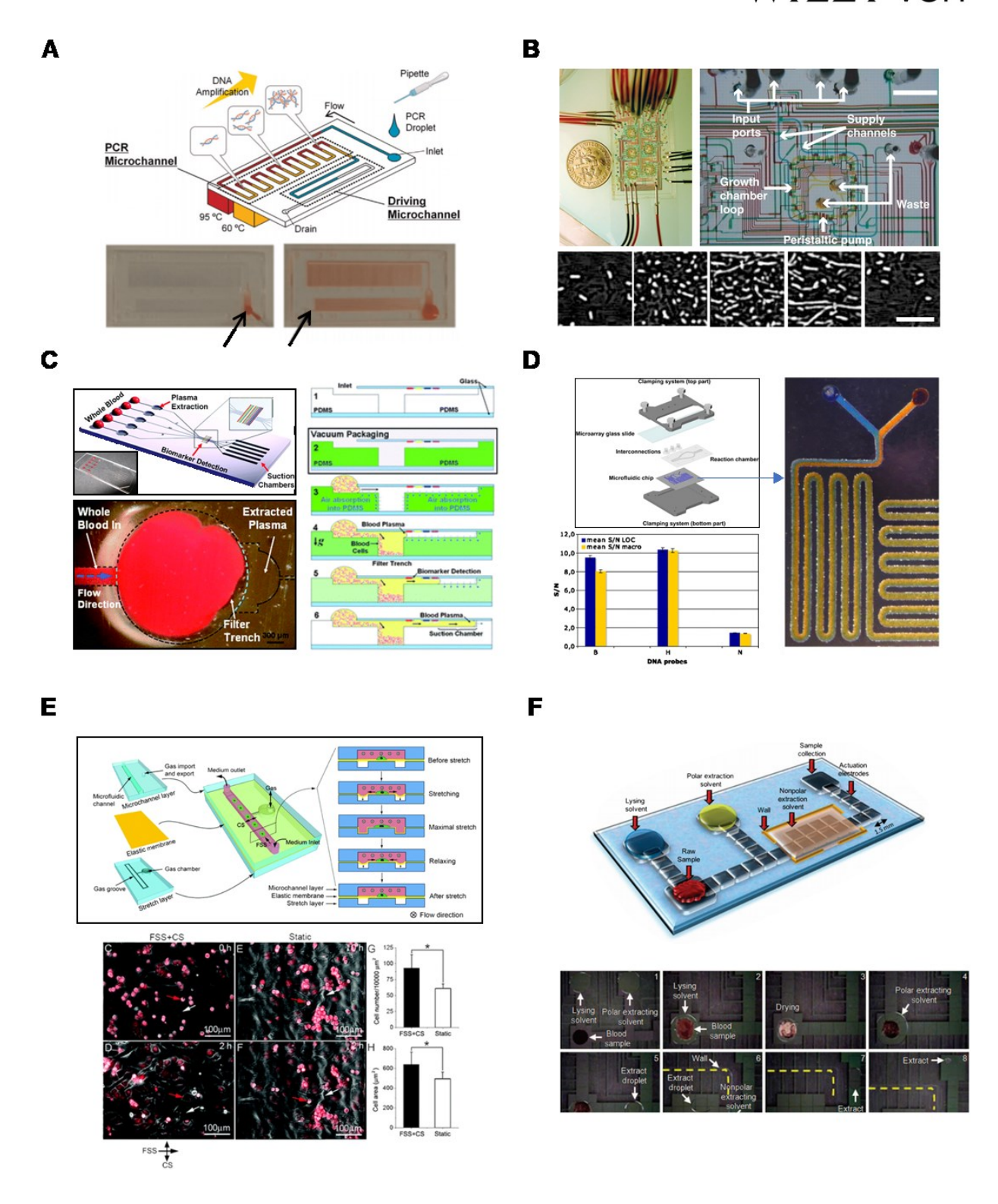


Figure 8. Applications of microfluidic devices in sample treatments. **A.** Disposable microfluidic polymerase chain reaction (PCR) testing chip. The top figure shows a diagram of the self-propelled

capillary flow chip with three different temperature zones. The bottom figures show the PCR running cycle with the flow moving from inlet to outlet. Reproduced with permission. [132] Copyright 2015, Elsevier. B. Microfluidic combining PCR flow and DNA hybridization for bacteria detection. Two left figures show the schematic and fabrication of the hybridization section of the chips. The right figure shows the hybridization result of the chip. Reproduced with permission. [133] Copyright 2014, Elsevier. C. Microfluidic chip that performs on-chip removal of red and white cells and analyte detection in platelet-containing plasma. The top left is a schematic with a volume metering section, filter trench, multiple biomarker detection channels, and suction chambers. The bottom left figure is a picture of the filter trench (cylindrical cavity). The right figure is a schematic of the device throughout blood plasma preparation. Reproduced with permission.^[134] Copyright 2011, Royal Society of Chemistry. **D.** Droplet based microfluidic extraction and quantification of estradiol in core needle biopsy samples of breast tissue. The top figure is a schematic of the device with eight reservoirs. The bottom figure is a collection of frames with the key steps in the extraction of estradiol. Reproduced with permission. [135] Copyright 2017, Royal Society of Chemistry. E. Microfluidic flow-stretch chip integrating fluid shear stress (FSS) and cyclic stretch (CS). The top figure is a schematic of the chip with a microchannel, elastic membrane, and stretch layer, as well as the cross-sectional operation of the three layers. The bottom figure shows vascular cells in the chip under static, FSS, CS, and FSS+CS conditions. Bottom bar graphs show the number of cells and their spread areas when affected by the FSS+CS condition. Reproduced with permission. [136] Copyright 2012, Royal Society of Chemistry. F. Microfluidic bioreactor that enables long-term culture and optical imaging and drug delivery. The top left figure shows the schematic of a single bioreactor with a culture heating and imaging window. The top right figure shows one of the bioreactors in action with organoids being deployed directly into the microfluidic channels. Bottom panels show time lapsed images of brain organoid ventricular zones. Reproduced with permission.^[137] Copyright 2021, American Institute of Physics.

4.3. Disease diagnosis by sensing and detection of biomarkers

The defining part of a microfluidic biomedical application is the ability to detect biomarkers. Biomarkers can be defined as accurate and reproducible medical indicators that can be

observed.[138] Biomarker detection with microfluidic channels can lead to rapid analysis. For instance, human chorionic gonadotropin (hCG) is a chemical created by trophoblast tissue and has been used to identify pregnancy states as well as a variety of cancers including choriocarcinoma. [139] Numbers of microfluidic devices have been developed. These devices prove to test hCG biomarkers utilizing microdroplets and colorimetric data in combination with a multicolor fluorescence detector. [140] Figure 9A shows a point of care immunosensor. It uses a polysilicon nanogap electrode which is connected to microfluidics channels provides amperometric characteristics and sensitivity data for the immunosensor. Another important biomarker is cholesterol. It is often carried in plasma by proteins such as low-density lipoprotein (LDL) and high density lipoprotein (HDL), and is harmful to heart and vascular diseases. [141] One way to measure cholesterol is through an oxidation reaction catalyzed by Horseradish Peroxidase (HRP) which produces colorimetric results.^[142] Figure 9B shows a point-of-care electrochemical cholesterol monitoring microfluidic device. The device uses a three-electrode system, PDMS microchannels, a sample syringe pump, and a potentiostat to measure voltage between electrodes. Samples of cholesterol are allowed to flow over the electrodes and produce amperometric data and information about cholesterol concentrations. For another example, tumor necrosis factor alpha (TNF α) is an important biomarker in type II diabetes^[143], and its detection is the focal point of the microfluidic device. [144] Figure 9C shows an electrochemical biomarker detection device for TNFa using a sandwich immunoassay. The device uses polymeric fluidics for sample control, inlet and outlet syringe ports, and two working electrodes for electrochemical signal and qualitative testing with antibodies. Glucose is an essential part of homeostasis and can be broken down into energy in the form of ATP.^[145] However, high glucose can be a biomarker for glycosuria which is a symptom of diabetes found in body fluid. [146] A recent wearable epidermal patch for sweat collection comes with pH and temperature corrected glucose results.^[147] Figure 9D shows a paper microfluidic device used for the detection of glucose in urine. The paper is printed to create millimeter-sized channels, bounded by a hydrophobic polymer to act as a low-cost point of care bioassay. The device absorbs the fluid (urine) on photoresist patterned chromatography paper which leads to the colorimetric results based on the concentration of reagents in glucose.

The field of microfluidics has expanded to include wearable devices for point of care applications. For one example, complete blood counts are important because they help to evaluate and diagnose health conditions, such as anemia, leukemia, infections, and allergic conditions.^[148]

The acquisition of blood counts is limited to a laboratory professional testing with expensive and bulky equipment. A microfluidics device has been developed to count CD3+ T-lymphocytes and CD19+ in whole blood samples for disease detection. [149] Figure 9E shows a wearable circuit wristband for blood counting and analysis. This device uses a flexible circuit and microfluidic channels paired with electrodes which would trigger a voltage spike during the pass of blood cells and thus provide a count. It could also be adapted to detect other substances using its mobile device software and deploying user specified biomarkers. Biomarkers in the composition of sweat can be used to detect a multitude of health issues such as ischemia through lactate, diabetes with glucoselevel in sweat and blood, and cystic fibrosis in chloride levels.^[150] Sweat can be used to keep active monitoring of cortisol, ascorbic acid (vitamin C), and galvanic sweat response (GSR) as seen in other skeletal microfluidic devices.^[151] To achieve these objectives, a recent sweat collecting device has been fabricated to be battery-free and fully self-powered by motion for similar biomarker detection, [152] as shown in Figure 9F. It is a wearable microfluidic device and composed of a stack of three subsystems: a skin adhesive layer for the area of sweat collection, colorresponsive materials in soft microfluidic channels for colorimetric analysis of sweat, and electronics for connection to devices. This device proves to capture and store sweat to measure lactate, glucose, chloride ion concentrations, and pH. These examples are a glimpse of microfluidic devices integrated with wearable electronics and their seamless integration is expected to be the future for the development of wearable, multifunctional microfluidic biomedical devices.

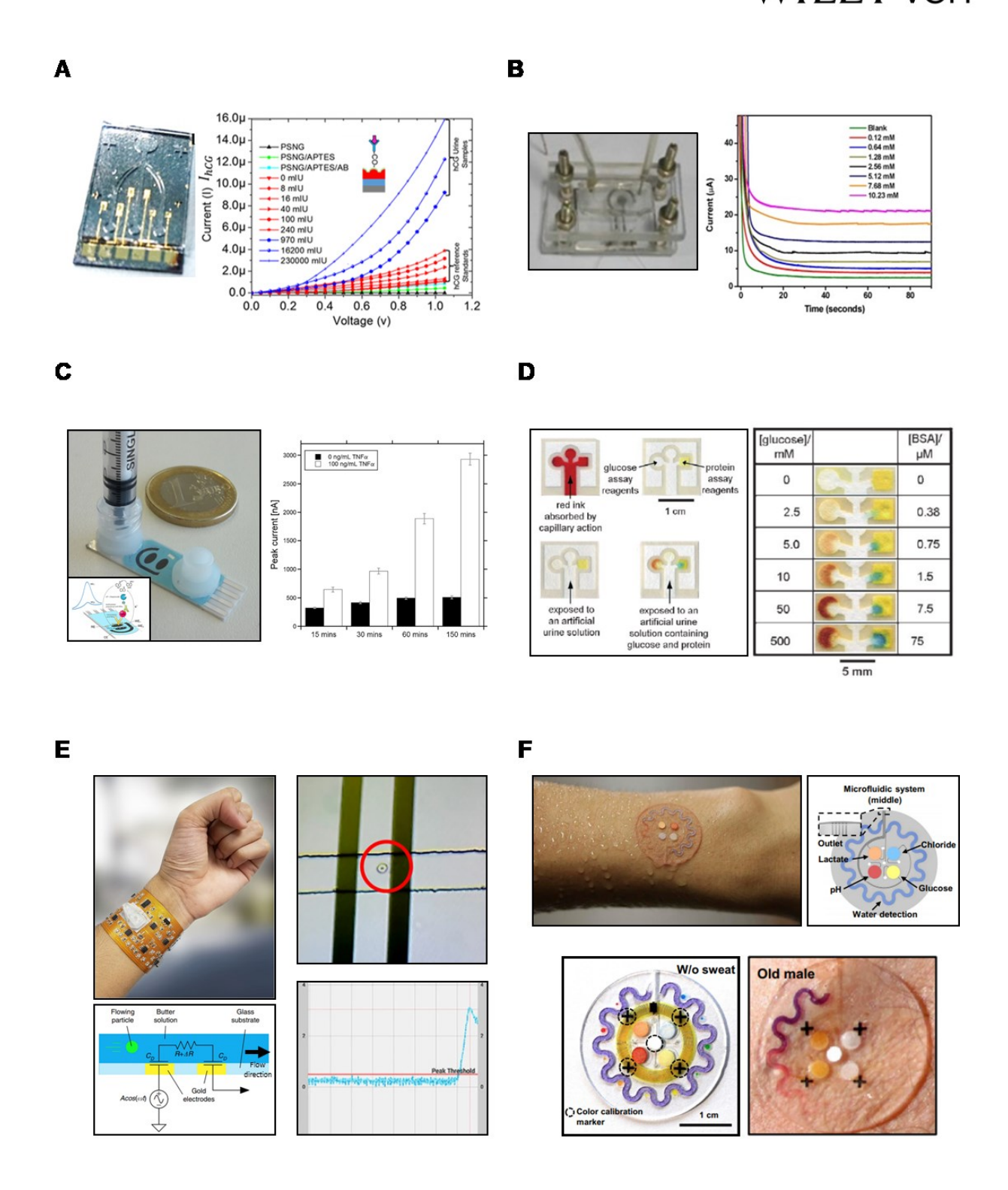


Figure 9. Sensing and detection applications of microfluidic devices. **A.** Point-of-Care Immunosensor for Human Chorionic Gonadotropin (hCG) in clinical urine. The left figure shows the actual device with electrodes connected to microfluidic channels. The right graph shows the

results of DC amperometric detection of urine samples against standard reference samples based on electrical capacitance measurements. Reproduced under terms of the CC-BY license. [153] Copyright 2015, The Authors, published by Plos One. B. Point-of-care electrochemical cholesterol monitoring microfluidic device. The left figure is a picture of the device with a three-electrode system and PDMS microchannels syringe pump and potentiostat connect to. The right graph shows different cholesterol concentrations with amperometric curves from the device with three microchannels. Reproduced with permission. [154] Copyright 2018, Elsevier. C. Electrochemical immunosensor for biomarker detection of tumor necrosis factor alpha (TNFa). The left figure is a schematic of the biochip with a modified electrode. The right graph shows the specificity of the immunoassay through Differential Pulse Voltammetry (DPV) when different antibodies were placed on the electrode. Reproduced with permission. [155] Copyright 2015, Elsevier. D. Paper microfluidic device for the determination of glucose in urine. The left figure shows the schematic diagram of the chromatography paper. The right figure shows colorimetric results of glucose detection assays with different concentrations of samples. Reproduced with permission.^[156] Copyright 2019, Springer Nature. E. Wearable microfluidic impedance cytometer on a wristband for portable biomarker counting and analysis. The top left figure is a picture of the flexible circuit device being worn. The bottom left figure shows the schematic of the microfluidic channel with relevant resistor and capacitor locations. The top right figure shows a blood drop, lubricated with Poly(ethylene glycol)-based polymer, flowing through the channel across an electrode. The bottom right graph shows the digital data plotted on a smartphone as human red blood cells flow past the electrodes. Reproduced under terms of the CC-BY license. [157] Copyright 2018, The Authors, published by Springer Nature. F. Wearable microfluidic device for the capture, storage, and colorimetric sensing of sweat. The top left figure shows the device being worn on the skin. The top right figure is a schematic of the middle microfluidic channel system, and four sections of reagents for colorimetric analysis (lactate, chloride, glucose, and pH). The bottom left figure shows the device stationary without any sweat to analyze in its normal state. The bottom right figure shows the device in use on an old male with the lactate and pH colorimetric sections. Reproduced with permission.^[10a] Copyright 2016, American Association for the Advancement of Science.

5. Summary and outlook

Micro/nanofluidics enabled devices and systems have attracted and will surely continue to attract numerous applications in biomedical engineering and healthcare monitoring and diagnoses with unprecedented functionalities, as they become more easily accessible and customizable with the emergence of advanced concepts of structural designs and manufacturing technologies in a combination of novel materials. For example, structural design has radically evolved from the early 2D channels to recent 3D channels toward multifunctionalities of bimolecular detection, separation, and mixture. Outer power sources that drive fluid transports have changed from the direct application of mechanical pressure and heat to magnetic or optical fields toward the achievement of wireless remote control. The requirement of soft materials that can conform to the trend of wearable technologies for in situ biomedical applications has led to the changes of manufacturing approaches from early casting, molding, and lithography to additive manufacturing such as 3D printing.

Going forward, the increasing demand for biomedical devices calls for new design and manufacturing concepts and strategies of elaborate, low-cost, and user-friendly micro/nanofluidic devices with multifunctionalities and wearable features^[158]. Devices with 3D channel patterns and spatial structures across scales are expected for monitoring multiple types of diseases and treatment monitoring of relevance to rich biofluids in the human body. Besides, 3D fluidic devices offer a unique situation that allows to observe in vitro interactions of biofluids with medicine molecules by mimicking biofluidic structures of the human body in treatments. For instance, the treatment of cancer typically requires long-term, high-cost surgery, radiation, medications, and other therapies, and 3D fluidic devices with multifunctionalities could be a potential candidate to serve inside our bodies.^[159] In parallel, soft materials are increasingly used due to their mechanical flexibility and lightweight that aligns with the intrinsic soft properties of human organs, the associated design principles and concepts for soft micro/nanofluidic biomedical devices need to be developed. The designs can start with traditional strategies of micro/nanochannels across dimensions with various material functional treatments that interact with components and molecules in biofluids. The channels and pores in soft materials could also be achieved by leveraging the large mechanical deformation properties of soft materials such as structural collapses with well pre-designs. In particular, the employment of smart soft materials that is responsive to external stimuli such as mechanical, temperature, electrical, or magnetic fields will yield programmable fluidic biomedical devices toward a precise, remote, and off-site control to measurement timing, location as well as

subject. More importantly, fabrication and manufacturing technologies of micro/nanofluidic

devices that are capable of accommodating the design from planar to complex steric 3D structures

are highly needed, where the continuous improvements of additive manufacturing such as 3D

printing are expected to lay a foundation. In addition, the manufacturing capability of multiphased

materials including responsive smart materials will be crucial for achieving a seamless integration

of structural design and manufacturing of micro/nanofluidic devices and systems across scales for

meeting desirable biomedical and healthcare monitoring applications.

Acknowledgment

M. Y. and Z. A. K. contributed equally to this work. This work is supported by the National Science

Foundation Directorate for Engineering Division of Chemical, Bioengineering, Environmental and

Transport Systems (Grant #1805451).

Received: ((will be filled in by the editorial staff))

Revised: ((will be filled in by the editorial staff))

Published online: ((will be filled in by the editorial staff))

37

References

- [1] a) R. Li, L. Wang, L. Yin, *Materials* **2018**, 11; b) S. S. Athukorala, T. S. Tran, R. Balu, V. K. Truong, J. Chapman, N. K. Dutta, N. Roy Choudhury, *Polymers* **2021**, 13, 474.
- [2] a) Y. H. Jung, J. U. Kim, J. S. Lee, J. H. Shin, W. Jung, J. Ok, T. i. Kim, *Adv. Mater.* 2020, 32, 1907478; b) R. A. Surmenev, R. V. Chernozem, I. O. Pariy, M. A. Surmeneva, *Nano Energy* 2021, 79, 105442.
- [3] a) Z. Ren, Y. Chang, Y. Ma, K. Shih, B. Dong, C. Lee, Adv. Opt. Mater. 2020, 8, 1900653;
 b) J. M. Rothberg, T. S. Ralston, A. G. Rothberg, J. Martin, J. S. Zahorian, S. A. Alie, N. J. Sanchez, K. Chen, C. Chen, K. Thiele, Proc. Natl. Acad. Sci. U. S. A. 2021, 118; c) M. Kumar, S. Yadav, A. Kumar, N. N. Sharma, J. Akhtar, K. Singh, Biosens. Bioelectron. 2019, 142, 111526; d) J. Yunas, B. Mulyanti, I. Hamidah, M. Mohd Said, R. E. Pawinanto, W. A. F. Wan Ali, A. Subandi, A. A. Hamzah, R. Latif, B. Yeop Majlis, Polymers 2020, 12, 1184.
- [4] a) J. Kim, A. S. Campbell, B. E. F. de Ávila, J. Wang, *Nat. Biotechnol.* 2019, 37, 389; b)
 G. Seo, G. Lee, M. J. Kim, S. H. Baek, M. Choi, K. B. Ku, C. S. Lee, S. Jun, D. Park, H.
 G. Kim, *ACS Nano* 2020, 14, 5135; c) H. U. Chung, A. Y. Rwei, A. Hourlier Fargette, S.
 Xu, K. Lee, E. C. Dunne, Z. Xie, C. Liu, A. Carlini, D. H. Kim, *Nat. Med.* 2020, 26, 418.
- [5] a) Y. Jiang, K. Dong, X. Li, J. An, D. Wu, X. Peng, J. Yi, C. Ning, R. Cheng, P. Yu, Adv. Funct. Mater. 2021, 31, 2005584; b) K. Kwon, H. Wang, J. Lim, K. San Chun, H. Jang, I. Yoo, D. Wu, A. J. Chen, C. G. Gu, L. Lipschultz, Proc. Natl. Acad. Sci. U. S. A. 2021, 118; c) Y. Cho, S. Park, J. Lee, K. J. Yu, Adv. Mater. 2021, 2005786.
- [6] a) B. Selvakumar, A. Kathiravan, *Talanta* **2021**, 122733; b) H. K. Balakrishnan, E. H. Doeven, A. Merenda, L. F. Dumée, R. M. Guijt, *Anal. Chim. Acta* **2021**, 338796.
- [7] a) A. Manz, D. J. Harrison, E. M. Verpoorte, J. C. Fettinger, A. Paulus, H. Lüdi, H. M. Widmer, *J. Chromatogr. A* 1992, 593, 253; b) M. U. Kopp, A. J. Mello, A. Manz, *Science* 1998, 280, 1046; c) A. Salman, H. Carney, S. Bateson, Z. Ali, *Talanta* 2020, 207, 120303.
- [8] a) J. Zhou, A. V. Ellis, N. H. Voelcker, *Electrophoresis* 2010, 31, 2; b) A. W. Auner, K.
 M. Tasneem, D. A. Markov, L. J. McCawley, M. S. Hutson, *Lab Chip* 2019, 19, 864.
- [9] a) S. N. Bhatia, D. E. Ingber, *Nat. Biotechnol.* 2014, 32, 760; b) R. Novak, M. Ingram, S. Marquez, D. Das, A. Delahanty, A. Herland, B. M. Maoz, S. S. Jeanty, M. R. Somayaji, M. Burt, *Nat. Biomed. Eng.* 2020, 4, 407.

- [10] a) A. Koh, D. Kang, Y. Xue, S. Lee, R. M. Pielak, J. Kim, T. Hwang, S. Min, A. Banks, P. Bastien, Sci. Transl. Med. 2016, 8, 366ra165; b) J. Choi, A. J. Bandodkar, J. T. Reeder, T. R. Ray, A. Turnquist, S. B. Kim, N. Nyberg, A. Hourlier Fargette, J. B. Model, A. J. Aranyosi, ACS Sens. 2019, 4, 379.
- [11] F. Ahmadi, K. Samlali, P. Q. N. Vo, S. C. C. Shih, Lab Chip 2019, 19, 524.
- [12] L. Bocquet, Nat. Mater. 2020, 19, 254.
- [13] M. Campisi, Y. Shin, T. Osaki, C. Hajal, V. Chiono, R. D. Kamm, *Biomaterials* 2018, 180, 117.
- [14] a) S. S. Bale, J. T. Borenstein, *Drug Metab Dispos* 2018, 46, 1638; b) J. Dai, Y. Xing, L. Xiao, J. Li, R. Cao, Y. He, H. Fang, A. Periasamy, J. Oberhozler, L. Jin, J. P. Landers, Y. Wang, X. Li, *ACS Biomater. Sci. Eng.* 2019, 5, 2041.
- [15] a) J. Zhang, S. Yan, D. Yuan, G. Alici, N. T. Nguyen, M. E. Warkiani, W. Li, *Lab Chip* 2016, 16, 10; b) P. H. Tsou, P. H. Chiang, Z. T. Lin, H. C. Yang, H. L. Song, B. R. Li, *Lab Chip* 2020, 20, 4007; c) L. Yin, W. Y. Au, C. C. Yu, T. Kwon, Z. Lai, M. Shang, M. E. Warkiani, R. Rosche, C. T. Lim, J. Han, *Biotechnol. Bioeng.* 2021, 118, 1951.
- [16] a) N. Kimura, M. Maeki, Y. Sato, Y. Note, A. Ishida, H. Tani, H. Harashima, M. Tokeshi, ACS Omega 2018, 3, 5044; b) J. Nam, J. Yoon, H. Jee, W. S. Jang, C. S. Lim, Adv. Mater. Technol. 2020, 5, 2000612.
- [17] B. Zhang, A. Korolj, B. F. L. Lai, M. Radisic, Nat. Rev. Mater. 2018, 3, 257.
- [18] a) A. Ortega Prieto, J. Skelton, S. Wai, E. Large, M. Lussignol, G. Vizcay Barrena, D. Hughes, R. Fleck, M. Thursz, M. Catanese, *Nat. Commun.* 2018, 9, 1; b) Y. Jun, J. Lee, S. Choi, J. H. Yang, M. Sander, S. Chung, S. H. Lee, *Sci. Adv.* 2019, 5, eaax4520; c) S. Lee, S. Kim, D. J. Koo, J. Yu, H. Cho, H. Lee, J. M. Song, S. Y. Kim, D. H. Min, N. L. Jeon, *ACS Nano* 2020, 15, 338; d) X. Wang, Y. Yu, C. Yang, C. Shao, K. Shi, L. Shang, F. Ye, Y. Zhao, *Adv. Funct. Mater.* 2021, 2105190.
- [19] V. L. Kopparthy, N. D. Crews, J. Microelectromech. Syst. 2018, 27, 434.
- [20] M. Rafeie, J. Zhang, M. Asadnia, W. Li, M. E. Warkiani, *Lab Chip* **2016**, 16, 2791.
- [21] Z. Chen, K. Memon, Y. Cao, G. Zhao, *Microsyst. Nanoeng.* **2020**, 6, 1.
- [22] D. Huh, B. D. Matthews, A. Mammoto, M. Montoya Zavala, H. Y. Hsin, D. E. Ingber, *Science* **2010**, 328, 1662.

- [23] C. Blundell, Y. S. Yi, L. Ma, E. R. Tess, M. J. Farrell, A. Georgescu, L. M. Aleksunes, D. Huh, *Adv. Healthcare Mater.* **2018**, 7, 1700786.
- [24] A. W. Martinez, S. T. Phillips, G. M. Whitesides, *Proc. Natl. Acad. Sci. U. S. A.* **2008**, 105, 19606.
- [25] C. Yeung, S. Chen, B. King, H. Lin, K. King, F. Akhtar, G. Diaz, B. Wang, J. Zhu, W. Sun, *Biomicrofluidics* **2019**, 13, 064125.
- [26] a) C. Y. Lee, C. L. Chang, Y. N. Wang, L. M. Fu, Int. J. Mol. Sci. 2011, 12, 3263; b) S. Jayaraj, S. Kang, Y. K. Suh, J. Mech. Sci. Technol. 2007, 21, 536; c) S. G. Kandlikar, J. Heat Transfer 2012, 134.
- [27] Ö. Baltekin, A. Boucharin, E. Tano, D. I. Andersson, J. Elf, *Proc. Natl. Acad. Sci. U. S. A.*2017, 114, 9170.
- [28] a) D. Valikhani, J. M. Bolivar, M. Viefhues, D. N. McIlroy, E. X. Vrouwe, B. Nidetzky, ACS Appl. Mater. Interfaces 2017, 9, 34641; b) H. Zhang, Y. Yang, X. Li, Y. Shi, B. Hu, Y. An, Z. Zhu, G. Hong, C. J. Yang, Lab Chip 2018, 18, 2749; c) C. Chen, Y. Liu, Z. Zheng, G. Zhou, X. Ji, H. Wang, Z. He, Anal. Chim. Acta 2015, 880, 1.
- [29] a) S. H. Tan, B. Semin, J. C. Baret, *Lab Chip* 2014, 14, 1099; b) R. Q. Zhang, S. L. Hong,
 C. Y. Wen, D. W. Pang, Z. L. Zhang, *Biosens. Bioelectron.* 2018, 100, 348.
- [30] H. Takahashi, T. Yasui, H. Kashida, K. Makino, K. Shinjo, Q. Liu, T. Shimada, S. Rahong, N. Kaji, H. Asanuma, Y. Baba, *Nanotechnology* 2021, 32.
- [31] L. Y. Yeo, J. R. Friend, Annu. Rev. Fluid Mech. 2014, 46, 379.
- [32] Y. Yang, K. Gupta, K. L. Ekinci, *Proc. Natl. Acad. Sci. U. S. A.* **2020**, 117, 10639.
- [33] K. J. Son, P. Gheibi, G. Stybayeva, A. Rahimian, A. Revzin, *Microsyst. Nanoeng.* **2017**, 3, 1.
- [34] J. Li, Z. Liu, H. Huang, H. C. Shum, *Micromachines* **2015**, 6, 1459.
- [35] S. A. Khashan, S. Dagher, A. Alazzam, B. Mathew, A. Hilal Alnaqbi, *J. Micromech. Microeng.* **2017**, 27, 055016.
- [36] M. Yin, L. Xiao, Q. Liu, S. Y. Kwon, Y. Zhang, P. R. Sharma, L. Jin, X. Li, B. Xu, *Adv. Healthcare Mater.* **2019**, 8, 1901170.
- [37] F. Guo, Z. Mao, Y. Chen, Z. Xie, J. P. Lata, P. Li, L. Ren, J. Liu, J. Yang, M. Dao, *Proc. Natl. Acad. Sci. U. S. A.* **2016**, 113, 1522.

- [38] D. J. Harrison, K. Fluri, K. Seiler, Z. Fan, C. S. Effenhauser, A. Manz, Science 1993, 261, 895.
- [39] M. Stjernström, J. Roeraade, J. Micromech. Microeng. 1998, 8, 33.
- [40] M. F. Ashby, *Materials selection in mechanical design*, Butterworth-Heinemann, Amsterdam, Netherlands **2017**.
- [41] R. Budynas, K. Nisbett, J. E. Shigley, *Shigley's mechanical engineering design*, McGraw-Hill, New York City, NY, USA, **2020**.
- [42] S. Begolo, G. Colas, J. L. Viovy, L. Malaquin, *Lab Chip* **2011**, 11, 508.
- [43] E. W. Young, E. Berthier, D. J. Guckenberger, E. Sackmann, C. Lamers, I. Meyvantsson, A. Huttenlocher, D. J. Beebe, *Lab Chip* **2011**, 83, 1408.
- [44] D. Puchberger Enengl, C. Krutzler, F. Keplinger, M. J. Vellekoop, *Lab Chip* **2014**, 14, 378.
- [45] T. N. Le, V. A. Nguyen, G. L. Bach, L. D. Tran, H. H. Cao, Adv. Polym. Tech. 2020, 2020.
- [46] E. S. Fakunle, I. Fritsch, Anal. Bioanal. Chem. 2010, 398, 2605.
- [47] W. Dungchai, O. Chailapakul, C. S. Henry, Anal. Chem. 2009, 81, 5821.
- [48] R. Gao, J. Ko, K. Cha, J. H. Jeon, G. e. Rhie, J. Choi, A. J. DeMello, J. Choo, *Biosens*. *Bioelectron*. **2015**, 72, 230.
- [49] W. H. Grover, R. H. Ivester, E. C. Jensen, R. A. Mathies, *Lab Chip* **2006**, 6, 623.
- [50] K. L. Wlodarczyk, D. P. Hand, M. M. Maroto Valer, Sci. Rep. 2019, 9, 1.
- [51] W. Nawrot, K. Malecha, Sensors 2020, 20, 1745.
- [52] J. Luo, T. Dziubla, R. Eitel, Sens. Actuators, B 2017, 240, 392.
- [53] Y. T. Yeh, Z. Lin, S. Y. Zheng, M. Terrones, Sci. Rep. 2018, 8, 1.
- [54] J. H. Chua, R. E. Chee, A. Agarwal, S. M. Wong, G. J. Zhang, *Anal. Chem.* **2009**, 81, 6266.
- [55] D. M. Ratner, E. R. Murphy, M. Jhunjhunwala, D. A. Snyder, K. F. Jensen, P. H. Seeberger, *Chem. Commun.* **2005**, 578.
- [56] M. Editors, Stainless Steel Microneedles for Flu Vaccine Delivery, https://www.medgadget.com/2009/04/stainless_steel_microneedles_for_flu_vaccine_delivery.html, accessed: 08/29, 2021.
- [57] H. de Puig, I. Bosch, L. Gehrke, K. Hamad Schifferli, *Trends Biotechnol.* 2017, 35, 1169.
- [58] Y. Xia, G. M. Whitesides, Angew. Chem. Int. Ed. Engl. 1998, 37, 550.
- [59] a) J. C. McDonald, G. M. Whitesides, *Acc. Chem. Res.* 2002, 35, 491; b) V. C. Pinto, P. J.
 Sousa, V. F. Cardoso, G. Minas, *Micromachines* 2014, 5, 738.

- [60] a) C. Linghu, S. Zhang, C. Wang, J. Song, npj Flexible Electron. 2018, 2, 1; b) C. Adamopoulos, A. Gharia, A. Niknejad, V. Stojanović, M. Anwar, Biosensors 2020, 10, 177; c) Y. Huang, Natl. Sci. Rev. 2020, 7, 558.
- [61] R. M. N. Lintag, F. G. D. Leyson, M. S. B. Matibag, K. J. R. Yap, *Mater. Today: Proc.* 2020, 22, 185.
- [62] a) Y. Zhang, Q. Liu, B. Xu, Extreme Mech. Lett. 2017, 16, 33; b) D. S. Wie, Y. Zhang, M. K. Kim, B. Kim, S. Park, Y.-J. Kim, P. P. Irazoqui, X. Zheng, B. Xu, C. H. Lee, Proc. Natl. Acad. Sci. U. S. A. 2018, 115, E7236; c) B. Kim, J. Jeon, Y. Zhang, D. S. Wie, J. Hwang, S. J. Lee, D. E. Walker Jr, D. C. Abeysinghe, A. Urbas, B. Xu, Nano Lett. 2019, 19, 5796; d) Y. Zhang, B. Kim, Y. Gao, D. S. Wie, C. H. Lee, B. Xu, Int. J. Solids Struct. 2019, 180, 30.
- [63] Y. Zhang, M. Yin, Y. Baek, K. Lee, G. Zangari, L. Cai, B. Xu, Proc. Natl. Acad. Sci. U. S. A. 2020, 117, 5210.
- [64] a) G. Li, S. Xu, *Mater. Des.* 2015, 81, 82; b) S.-H. Song, C.-K. Lee, T.-J. Kim, I.-c. Shin,
 S.-C. Jun, H.-I. Jung, *Microfluid. Nanofluid.* 2010, 9, 533; c) Y. Jia, J. Jiang, X. Ma, Y. Li,
 H. Huang, K. Cai, S. Cai, Y. Wu, *Sci. Bull.* 2008, 53, 3928.
- [65] a) V. Faustino, S. O. Catarino, R. Lima, G. Minas, J Biomech 2016, 49, 2280; b) N. C. Speller, G. G. Morbioli, M. E. Cato, T. P. Cantrell, E. M. Leydon, B. E. Schmidt, A. M. Stockton, Sens. Actuators, B 2019, 291, 250; c) A. T. Alsharhan, R. Acevedo, R. Warren, R. D. Sochol, Lab Chip 2019, 19, 2799.
- [66] A. A. Yazdi, A. Popma, W. Wong, T. Nguyen, Y. Pan, J. Xu, Microfluid. Nanofluid. 2016, 20, 50.
- [67] a) M. Padash, C. Enz, S. Carrara, Sensors 2020, 20; b) R. D. Sochol, E. Sweet, C. C. Glick,
 S. Y. Wu, C. Yang, M. Restaino, L. Lin, Microelectron. Eng. 2018, 189, 52.
- [68] N. Bhattacharjee, A. Urrios, S. Kang, A. Folch, *Lab Chip* **2016**, 16, 1720.
- [69] V. Saggiomo, A. H. Velders, Adv. Sci. 2015, 2, 1500125.
- [70] R. Sochol, E. Sweet, C. Glick, S. Venkatesh, A. Avetisyan, K. Ekman, A. Raulinaitis, A. Tsai, A. Wienkers, K. Korner, *Lab Chip* **2016**, 16, 668.
- [71] a) C. Tzivelekis, P. Sgardelis, K. Waldron, R. Whalley, D. Huo, K. Dalgarno, *PLoS One*2020, 15, e0240237; b) A. P. Kuo, N. Bhattacharjee, Y. S. Lee, K. Castro, Y. T. Kim, A. Folch, *Adv. Mater. Technol.* 2019, 4.

- [72] N. P. Macdonald, J. M. Cabot, P. Smejkal, R. M. Guijt, B. Paull, M. C. Breadmore, *Anal. Chem.* **2017**, 89, 3858.
- [73] D. I. Walsh III, D. S. Kong, S. K. Murthy, P. A. Carr, *Trends Biotechnol.* **2017**, 35, 383.
- [74] H. Kim, H. S. Lee, Y. Jeon, W. Park, Y. Zhang, B. Kim, H. Jang, B. Xu, Y. Yeo, D. R. Kim, ACS Nano 2020, 14, 7227.
- [75] F. R. de Souza, G. L. Alves, W. K. Coltro, Anal. Chem. 2012, 84, 9002.
- [76] Custompart.net, Fused Deposition Modeling (FDM), http://www.custompartnet.com/wu/fused-deposition-modeling, accessed: 08/29, 2021.
- [77] Custompart.net, Inkjet Printing, http://www.custompartnet.com/wu/ink-jet-printing, accessed: 08/29, 2021.
- [78] Custompart.net, Stereolithography, http://www.custompartnet.com/wu/stereolithography, accessed: 08/29, 2021.
- [79] S. Waheed, J. M. Cabot, N. P. Macdonald, T. Lewis, R. M. Guijt, B. Paull, M. Breadmore, *Lab Chip* 2016, 16, 1993.
- [80] R. F. Quero, G. D. Silveira, J. A. F. da Silva, D. P. de Jesus, *Lab Chip* **2021**.
- [81] A. D. Castiaux, C. W. Pinger, E. A. Hayter, M. E. Bunn, R. S. Martin, D. M. Spence, *Anal. Chem.* **2019**, 91, 6910.
- [82] J. Huang, Q. Qin, J. Wang, *Processes* **2020**, 8, 1138.
- [83] a) J. Park, M. J. Tari, H. T. Hahn, *Rapid Prototyping J.* **2000**; b) B. Dermeik, N. Travitzky, *Adv. Eng. Mater.* **2020**, 22, 2000256.
- [84] P. Prabhakar, R. Sen, N. Dwivedi, R. Khan, P. Solanki, A. Srivastava, C. Dhand, *Front. Nanotechnol* **2021**.
- [85] A. Z. Nelson, K. S. Schweizer, B. M. Rauzan, R. G. Nuzzo, J. Vermant, R. H. Ewoldt, *Curr. Opin. Solid State Mater. Sci.* **2019**, 23, 100758.
- [86] G. van der Velden, D. Fan, U. Staufer, *Micro Nano Eng.* **2020**, 7, 100054.
- [87] M. Bauer, L. Kulinsky, *Micromachines* **2018**, 9, 27.
- [88] H. Yang, J. C. Lim, Y. Liu, X. Qi, Y. L. Yap, V. Dikshit, W. Y. Yeong, J. Wei, *Virtual Phys. Prototyping* **2017**, 12, 95.
- [89] H. Gong, B. P. Bickham, A. T. Woolley, G. P. Nordin, *Lab Chip* **2017**, 17, 2899.
- [90] A. K. Au, W. Huynh, L. F. Horowitz, A. Folch, Angew. Chem., Int. Ed. 2016, 55, 3862.

- [91] R. Su, J. Wen, Q. Su, M. S. Wiederoder, S. J. Koester, J. R. Uzarski, M. C. McAlpine, *Sci. Adv.* **2020**, 6, eabc9846.
- [92] O. Vanderpoorten, Q. Peter, P. K. Challa, U. F. Keyser, J. Baumberg, C. F. Kaminski, T. P. Knowles, *Microsyst. Nanoeng.* 2019, 5, 1.
- [93] A. C. Lamont, A. T. Alsharhan, R. D. Sochol, Sci. Rep. 2019, 9, 394.
- [94] a) J. C. Eijkel, A. Van Den Berg, *Microfluid. Nanofluid.* **2005**, 1, 249; b) X. Chen, L. Zhang, *Sens. Actuators, B* **2018**, 254, 648.
- [95] R. Marie, J. N. Pedersen, K. U. Mir, B. Bilenberg, A. Kristensen, *Nanoscale* **2018**, 10, 1376.
- [96] C. Duan, W. Wang, Q. Xie, *Biomicrofluidics* **2013**, 7, 026501.
- [97] a) Y. Xu, Adv. Mater. 2018, 30, 1702419; b) K. Morikawa, Y. Kazoe, Y. Takagi, Y. Tsuyama, Y. Pihosh, T. Tsukahara, T. Kitamori, Micromachines 2020, 11, 995; c) D. Xia, J. Yan, S. Hou, Small 2012, 8, 2787.
- [98] a) K. Raidongia, J. Huang, J. Am. Chem. Soc. 2012, 134, 16528; b) S. Park, S. Hong, J. Kim, S. Y. Son, H. Lee, S. J. Kim, Sci. Rep. 2021, 11, 1.
- [99] Y. Lei, W. Wang, W. Wu, Z. Li, Appl. Phys. Lett. 2010, 96, 263102.
- [100] S. Shin, B. S. Kim, J. Song, H. Lee, H. H. Cho, *Lab Chip* **2012**, 12, 2568.
- [101] E. Choi, K. Kwon, S. J. Lee, D. Kim, J. Park, Lab Chip 2015, 15, 1794.
- [102] T. P. Ding, K. Liu, J. Li, G. B. Xue, Q. Chen, L. Huang, B. Hu, J. Zhou, Adv. Funct. Mater. 2017, 27.
- [103] M. Kim, D. Ha, T. Kim, Nat. Commun. 2015, 6, 1.
- [104] S. M. Park, Y. S. Huh, H. G. Craighead, D. Erickson, Proc. Natl. Acad. Sci. U. S. A. 2009, 106, 15549.
- [105] P. N. Nge, C. I. Rogers, A. T. Woolley, Chem. Rev. 2013, 113, 2550.
- [106] R. Epifania, R. R. Soares, I. F. Pinto, V. Chu, J. P. Conde, Sens. Actuators, B 2018, 265, 452.
- [107] S. Di Fraia, N. Massarotti, P. Nithiarasu, Int. J. Numer. Methods Heat Fluid Flow 2018.
- [108] a) H. Fallahi, J. Zhang, H. P. Phan, N. T. Nguyen, *Micromachines* **2019**, 10, 830; b) M. Sesen, C. J. Rowlands, *Microsyst. Nanoeng.* **2021**, 7, 1.
- [109] J. Hess, S. Zehnle, P. Juelg, T. Hutzenlaub, R. Zengerle, N. Paust, *Lab Chip* **2019**, 19, 3745.

- [110] L. Kong, A. Levin, Z. Toprakcioglu, Y. Xu, H. Gang, R. Ye, B. Z. Mu, T. P. Knowles, *Langmuir* **2020**, 36, 2349.
- [111] X. Yao, G. Zhu, P. Zhu, J. Ma, W. Chen, Z. Liu, T. Kong, Adv. Funct. Mater. 2020, 30, 1909389.
- [112] M. Bauer, M. Ataei, M. Caicedo, K. Jackson, M. Madou, L. Bousse, *Microfluid. Nanofluid.* **2019**, 23, 1.
- [113] T. Akyazi, L. Basabe Desmonts, F. Benito Lopez, Anal. Chim. Acta 2018, 1001, 1.
- [114] O. A. Ibrahim, M. A. Goulet, E. Kjeang, J. Electrochem. Soc. 2015, 162, F639.
- [115] C. Watson, S. Senyo, *HardwareX* **2019**, 5, e00063.
- [116] Y. Gao, M. Wu, Y. Lin, J. Xu, Lab Chip 2020, 20, 4512.
- [117] T. Glawdel, C. L. Ren, Mech. Res. Commun. 2009, 36, 75.
- [118] H. Kim, J. Kim, Microfluid. Nanofluid. 2014, 16, 623.
- [119] A. M. Klein, L. Mazutis, I. Akartuna, N. Tallapragada, A. Veres, V. Li, L. Peshkin, D. A. Weitz, M. W. Kirschner, *Cell* 2015, 161, 1187.
- [120] I. Jang, H. Kang, S. Song, D. S. Dandy, B. J. Geiss, C. S. Henry, *Analyst* **2021**, 146, 1932.
- [121] Q. Zhang, T. Wang, Q. Zhou, P. Zhang, Y. Gong, H. Gou, J. Xu, B. Ma, Sci. Rep. 2017, 7,1.
- [122] M. Tanyeri, C. M. Schroeder, *Nano Lett.* **2013**, 13, 2357.
- [123] a) J. J. Gooding, Electroynalysis (N.Y.N.Y.) 2002, 14, 1149; b) A. S. Lubbe, Q. Liu, S. J. Smith, J. W. De Vries, J. C. Kistemaker, A. H. De Vries, I. Faustino, Z. Meng, W. Szymanski, A. Herrmann, J. Am. Chem. Soc. 2018, 140, 5069.
- [124] S. H. Huang, Y. S. Chang, J. M. J. Juang, K. W. Chang, M. H. Tsai, T. P. Lu, L. C. Lai, E. Y. Chuang, N. T. Huang, *Analyst* 2018, 143, 1367.
- [125] S. C. Cowin, L. Cardoso, J. Biomech. 2015, 48, 842.
- [126] D. H. Kuan, C. C. Wu, W. Y. Su, N. T. Huang, Sci. Rep. 2018, 8, 1.
- [127] Z. Gu, M. L. Wu, B. Y. Yan, H. F. Wang, C. Kong, ACS Omega 2020, 5, 11196.
- [128] J. L. Garcia Cordero, S. J. Maerkl, Curr. Opin. Biotechnol. 2020, 65, 37.
- [129] S. Lehoux, in *Biomechanics of Coronary Atherosclerotic Plaque*, Academic Press, Waltham, MA **2021**, p. 49.
- [130] S. Mao, Q. Zhang, H. Li, W. Zhang, Q. Huang, M. Khan, J. M. Lin, Chem. Sci. 2018, 9, 7694.

- [131] E. Di Lullo, A. R. Kriegstein, Nat. Rev. Neurosci. 2017, 18, 573.
- [132] H. Tachibana, M. Saito, S. Shibuya, K. Tsuji, N. Miyagawa, K. Yamanaka, E. Tamiya, *Biosens. Bioelectron.* **2015**, 74, 725.
- [133] X. Jiang, N. Shao, W. Jing, S. Tao, S. Liu, G. Sui, *Talanta* **2014**, 122, 246.
- [134] I. K. Dimov, L. Basabe Desmonts, J. L. Garcia Cordero, B. M. Ross, A. J. Ricco, L. P. Lee, Lab Chip 2011, 11, 845.
- [135] S. Abdulwahab, A. H. Ng, M. D. Chamberlain, H. Ahmado, L. A. Behan, H. Gomaa, R. F. Casper, A. R. Wheeler, *Lab Chip* **2017**, 17, 1594.
- [136] W. Zheng, B. Jiang, D. Wang, W. Zhang, Z. Wang, X. Jiang, Lab Chip 2012, 12, 3441.
- [137] I. Khan, A. Prabhakar, C. Delepine, H. Tsang, V. Pham, M. Sur, *Biomicrofluidics* **2021**, 15, 024105.
- [138] D. S. Wishart, B. Bartok, E. Oler, K. Y. Liang, Z. Budinski, M. Berjanskii, A. Guo, X. Cao, M. Wilson, *Nucleic Acids Res.* **2021**, 49, D1259.
- [139] D. Betz, K. Fane, in *StatPearls* StatPearls Publishing, Treasure Island, FL **2020**.
- [140] P. Chen, Q. Sun, F. Xiong, H. Zhong, Z. Yao, Y. Zeng, *Biomicrofluidics* **2020**, 14, 024107.
- [141] M. J. Vincent, B. Allen, O. M. Palacios, L. T. Haber, K. C. Maki, Am. J. Clin. Nutr. 2019, 109, 7.
- [142] S. Karnik, C. Lee, A. Cancino, A. Bhushan, *Technology* **2018**, 6, 135.
- [143] M. S. H. Akash, K. Rehman, A. Liaqat, J. Cell. Biochem. 2018, 119, 105.
- [144] R. Rodriguez Moncayo, R. J. Jimenez Valdes, A. M. Gonzalez Suarez, J. L. Garcia Cordero, ACS Sens. 2020, 5, 353.
- [145] P. J. Hantzidiamantis, S. L. Lappin, in *StatPearls*, StatPearls Publishing, Treasure Island, FL **2021**.
- [146] J. Xiao, Y. Liu, L. Su, D. Zhao, L. Zhao, X. Zhang, Anal. Chem. 2019, 91, 14803.
- [147] A. Wiorek, M. Parrilla, M. Cuartero, G. n. A. Crespo, Anal. Chem. 2020, 92, 10153.
- [148] Y. M. Alomari, S. N. H. Sheikh Abdullah, R. Zaharatul Azma, K. Omar, *Comput. Math. Methods Med.* **2014**, 2014.
- [149] A. M. Noor, T. Masuda, W. Lei, K. Horio, Y. Miyata, M. Namatame, Y. Hayase, T. I. Saito, F. Arai, *Sens. Actuators, B* **2018**, 276, 107.
- [150] M. Chung, G. Fortunato, N. Radacsi, J. R. Soc., Interface 2019, 16, 20190217.

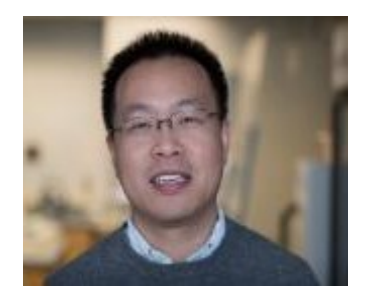
- [151] S. Kim, B. Lee, J. T. Reeder, S. H. Seo, S. U. Lee, A. Hourlier Fargette, J. Shin, Y. Sekine,
 H. Jeong, Y. S. Oh, *Proc. Natl. Acad. Sci. U. S. A.* 2020, 117, 27906.
- [152] Y. Song, J. Min, Y. Yu, H. Wang, Y. Yang, H. Zhang, W. Gao, Sci. Adv. 2020, 6, eaay9842.
- [153] S. Balakrishnan, U. Hashim, S. C. Gopinath, P. Poopalan, H. Ramayya, M. Iqbal Omar, R. Haarindraprasad, P. Veeradasan, *PLoS One* **2015**, 10, e0137891.
- [154] G. Kaur, M. Tomar, V. Gupta, Sens. Actuators, B 2018, 261, 460.
- [155] U. Eletxigerra, J. Martinez Perdiguero, S. Merino, Sens. Actuators, B 2015, 221, 1406.
- [156] H. Zhang, E. Smith, W. Zhang, A. Zhou, Biomed. Microdevices 2019, 21, 1.
- [157] A. Furniturewalla, M. Chan, J. Sui, K. Ahuja, M. Javanmard, *Microsyst. Nanoeng.* **2018**, 4, 1.
- [158] D. B. Weibel, G. M. Whitesides, Curr. Opin. Chem. Biol. 2006, 10, 584.
- [159] T. Wang, D. Wang, H. Yu, B. Feng, F. Zhou, H. Zhang, L. Zhou, S. Jiao, Y. Li, Nat Commun 2018, 9, 1532.



Mengtian Yin is a PhD candidate in the Department of Mechanical and Aerospace Engineering at the University of Virginia. He received his B.S. in Mechanical Engineering from North Carolina State University in 2016. Under the supervision of Prof. Baoxing Xu starting in 2018, his research focus is on mechanical design and nanomanufacturing of biomedical devices for healthcare monitoring.



Zachary Kim is a senior mechanical engineering undergraduate student at the University of Virginia. His research interests involve designing innovative energy generation systems as well as the biomechanics involved in wearable medical devices.



Baoxing Xu is currently an associate Professor in the Department of Mechanical and Aerospace Engineering at the University of Virginia. He received his PhD in Mechanics and Materials from Columbia University in 2012 and was a Beckman Postdoctoral Fellow at the University of Illinois at Urbana-Champaign from 2012 to 2014. His research interests are focused on mechanics-driven extreme design and nanomanufacturing of functional materials, structures and devices for applications in wearable electronics and healthcare, in particular, transfer printing in liquid,

solution shearing, soft-hard material integration, solid-liquid functionalized materials, and bioinspired devices and structures.

ToC figure (55 mm broad × 50 mm high):

Micro/nanofluidic devices and systems that allow to sense transported liquid offer an attractive platform in biomedical engineering and healthcare monitoring. The concepts and strategies of design and manufacturing that are crucial to achieve low-cost and user-friendly features of the devices and systems with multifunctionalities, together with the associated challenges and opportunities are discussed with representative biomedical applications.

Mengtian Yin, Zachary Alexander Kim, and Baoxing Xu*

Micro/nanofluidics enabled biomedical devices: Integration of structural design and manufacturing

